RESEARCH ARTICLE

Process Systems Engineering

Minimum reflux calculation for multicomponent distillation in multi-feed, multi-product columns: Mathematical model

Zheyu Jiang[1,2] | Mohit Tawarmalani[3] | Rakesh Agrawal[1]

[1]Davidson School of Chemical Engineering, Purdue University, West Lafayette, Indiana, USA

[2]School of Chemical Engineering, Oklahoma State University, Stillwater, Oklahoma, USA

[3]Krannert School of Management, Purdue University, West Lafayette, Indiana, USA

Correspondence

Zheyu Jiang, School of Chemical Engineering, Oklahoma State University, Stillwater, Oklahoma 74078, USA.
Email: zheyu.jiang@okstate.edu

Mohit Tawarmalani, Krannert School of Management, Purdue University, West Lafayette, Indiana 47907, USA.
Email: mtawarma@purdue.edu

Rakesh Agrawal, Davidson School of Chemical Engineering, Purdue University, West Lafayette, IN 47907, USA.
Email: agrawalr@purdue.edu

Funding information

U.S. Department of Energy, Grant/Award Number: DE-EE0005768

Abstract

Multi-feed, multi-product distillation columns are ubiquitous in multicomponent distillation systems. The minimum reflux ratio of a distillation column is directly related to its energy consumption and capital cost. Thus, it is a key parameter for distillation systems design, operation, and comparison. In this series, we present the first accurate shortcut based algorithmic method to determine the minimum reflux condition for any general multi-feed, multi-product (MFMP) distillation column separating any ideal multicomponent mixture. The classic McCabe-Thiele or Underwood method is a special case of this general approach. Compared with existing techniques, this method does not involve any rigorous tray-by-tray calculation, nor does it require guessing of key components. In this first part of the series, we present the mathematical model for a general MFMP column, derive constraints for feasible separation and minimum reflux condition, discuss their geometric interpretations, and present an illustrative example to demonstrate the effectiveness of our approach.

KEYWORDS

minimum reflux ratio, multicomponent distillation, multi-feed distillation column, multi-product distillation column, shortcut model

1 | INTRODUCTION

Distillation is an important separation process that accounts for 90%–95% of all liquid separations and consumes more than 40% of energy in the chemical and refining industries.[1,2] While alternative separation technologies are under development and testing, the predominance of distillation is unlikely to change at least in the near future for a number of industrial applications due to its inimitable technical advantages and economic attractiveness.[3–6] To separate a multicomponent mixture that contains n components into n pure products by distillation, a sequence of distillation columns known as a *distillation configuration* is generally required. Shah and Agrawal[7] successfully generated the complete search space of distillation configurations that use exactly $(n-1)$ columns for n-component mixture separation. Figure 1

shows two of the 152 distinct distillation configurations for separating a four-component mixture derived from Shah and Agrawal's method.[7] It turns out that most configurations in this search space contain at least one distillation column with multiple feed streams and/or one or more side-stream withdrawals.[9] In addition, compared to configurations that use only *simple columns* each with exactly one feed and two product streams (e.g., Figure 1A), it has been shown that configurations involving one or more multi-feed, multi-product (MFMP) columns (e.g., Figure 1B) often lead to significant energy and capital cost savings.[9] These MFMP columns have been widely used in industrial applications such as crude oil fractionation, air separation, extractive distillation, multi-effect distillation, and so on. To design these distillation systems effectively, process engineers need to fundamentally understand how the internal liquid and vapor traffic within an MFMP
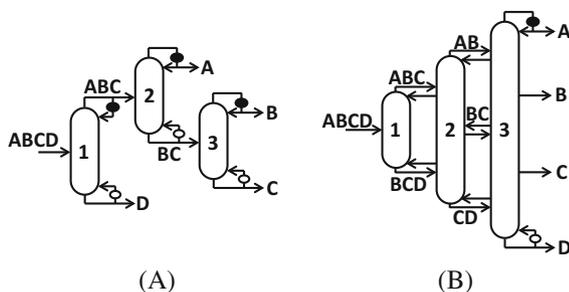
FIGURE 1 (A) A four-component configuration containing only simple columns; (B) the well-known fully thermally coupled configuration[8] in which columns 2 and 3 are both MFMP columns. Here and thereafter, letters *A*, *B*, *C*, and so on represent pure components with their volatilities decreasing in alphabetical order. Also, we indicate reboilers by open circles and condensers by filled circles.

column affects product quality, including the column's minimum reflux condition.

The minimum reflux ratio of a distillation column, which directly translates to its reboiler vapor duty requirement at minimum reflux condition, is an important parameter that provides key information on the column's optimal design and operation. With the knowledge of minimum reflux ratio, process engineers can estimate the actual heat duty requirement of the distillation column in operation.[10,11] The minimum reflux ratio also serves as a direct indicator for the capital cost of a distillation column, as it is closely related to the number of stages, column diameter and height, as well as reboiler and condenser sizes.[12–14] Because of these reasons, the minimum reflux ratio has been commonly chosen as the objective function for optimizing, comparing, and ranklisting different distillation column designs.[9,15–19] As a result, a fast and accurate determination of the minimum reflux ratio or minimum reboiler vapor duty requirement is crucial for synthesizing and designing attractive multicomponent distillation systems, and failing to do so often leads to inefficient and unnecessarily large columns being built and operated.

Over the past decades, a number of attempts have been made to identify the true minimum reflux condition for MFMP columns that carry out ideal/near ideal, nonideal, or even azeotropic mixture separations. These attempts led to the development of various *shortcut*, *geometric*, or *rigorous* methods. Most rigorous methods involve detailed tray-by-tray calculations by simultaneously solving the so-called MESH equations which incorporate mass and energy balances as well as phase equilibrium relations.[20–24] These methods are now embedded in process simulation tools such as Aspen Plus. However, as the number of components involved increases, these tray-by-tray calculations quickly become too computationally expensive to be performed in a global optimization framework, in which optimal operating conditions are to be identified for either one or the entire search space of configurations where each configuration consists of multiple columns.

In addition to rigorous methods, several geometric based approaches have also been proposed to address the minimum reflux

problem in an iterative manner. Lucia et al.[25] conducted a comprehensive literature survey summarizing these geometric methods. Among them, Levy and Doherty[26] made one of the earliest and most influential contributions by introducing first-order finite difference approximation followed by numerical integration to calculate the liquid composition profile for each column section in a multi-feed column separating ternary mixtures. In order for a separation to be feasible, composition profiles associated with any two adjacent column sections must be connected. In the extreme case of minimum reflux, composition profiles inside the *pinched* column sections barely touch each other. A column section is said to be pinched when there exists a region in which the liquid or vapor composition stays unchanged from tray to tray. Therefore, a pinched column section will require an infinite number of stages for separation. Subsequently, Koehler et al.[27] suggested a "minimum angle" criterion for minimum reflux condition in a simple column separating binary and ternary mixtures. This method is based on the observation that, when the column is operated under minimum reflux, the angle between the vector connecting feed composition and rectifying section pinch zone composition and the vector connecting feed composition and stripping section pinch zone composition is minimized. Later, Koehler et al.[28] extended this criterion to characterize the minimum reflux behavior for multi-product columns separating ternary mixtures. Nevertheless, the minimum angle criterion, which is generally formulated as a complex nonlinear programming (NLP) problem,[27] is computationally challenging to solve and lacks solid physical basis. Other geometric based approaches (e.g., "zero-volume" method, "separation driving force" method, and "rectification body" method) have also been proposed to calculate the minimum reflux ratio for nonideal or azeotropic multicomponent distillation in a simple column.[29–34] Although some of these methods have been extended to MFMP columns,[35–37] they still suffer from computational inefficiency and convergence issues due to model complexity and numerical instability. Moreover, while some of these methods work well for three- or four-component mixture separations where composition profiles can be visualized, generalizing them to separations involving higher number of components is tricky, and a clear generalization does not exist. To address these difficulties, there is a need to develop an accurate, robust shortcut based approach that does not require rigorous tray-by-tray calculations or tedious iterative procedures.
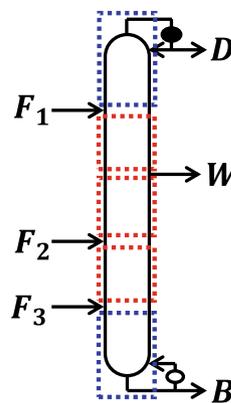
Most existing shortcut methods for estimating the minimum reflux ratio for multicomponent distillation in MFMP columns generalize the well-known Underwood method,[38,39] which was originally developed for simple columns. The Underwood method avoids the need for rigorous tray-by-tray calculations by making three major underlying assumptions: *ideal liquid–vapor equilibrium* (ideal-VLE), *constant relative volatility* (CRV), and *constant molar overflow* (CMO). As corollaries of these assumptions, all components have constant and equal latent heat of vaporization, and there is no enthalpy of mixing. Despite these simplifications, the minimum reflux ratio can be estimated with reasonable accuracy even for many nonideal[40] or azeotropic systems[41] that cover a wide range of industrially important separations.
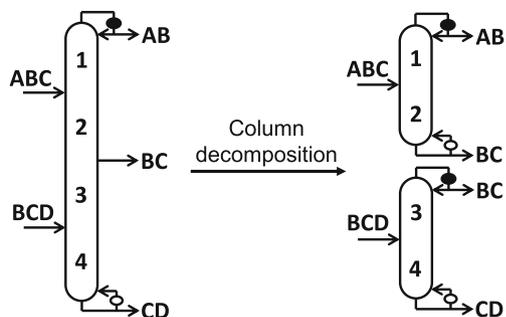
FIGURE 2 According to column decomposition, this two-feed, three-product column can be decomposed into two simple columns. Let $V_{\min}^{\text{Sec}\,2}$ and $V_{\min}^{\text{Sec}\,4}$ be the minimum reboiler vapor duties determined by the Underwood method for the upper and lower simple columns, respectively. Then, column decomposition postulates that the minimum reboiler vapor duty of this MFMP column is given by $\max\left\{V_{\min}^{\text{Sec}\,2} - V_{\text{BCD}}, V_{\min}^{\text{Sec}\,4}\right\}$, where V_{BCD} is the vapor portion flow rate of feed BCD.

FIGURE 3 A general MFMP column. The topmost and bottommost column sections are present in both simple columns and MFMP columns. However, the intermediate sections are unique to MFMP columns. Note that by considering a general column section as the smallest module of an MFMP column, our modeling framework is fundamentally different from the column decomposition method proposed by others.

One of the first generalizations of the Underwood method was derived by Barnes et al.[42] to study the minimum reflux behavior for multi-feed columns. Unfortunately, their solution procedure still requires extensive iterative calculations. Wachter et al.[43] modified the Underwood method to estimate the minimum reflux ratio for MFMP columns. However, the success of their method relies on correct identification of key components in the separation. In general, identifying the right key components is not a straightforward task for MFMP columns. Sugie and Lu[44] extended the Underwood method to multi-product columns with only saturated liquid sidedraws. They claimed that, at minimum reflux, such multi-product columns must be pinched at the feed location. Later, Glinos and Malone[45] derived shortcut design equations for columns with exactly one feed and one sidedraw stream. Nikolaides and Malone[46] further extended the work of Glinos and Malone[45] to general MFMP columns. They argued that an MFMP column could always be decomposed into a series of simple columns, each containing exactly one feed or sidedraw stream sandwiched by two column sections (see Figure 2). The classic Underwood method can then be applied to determine the minimum reflux ratio for each simple column generated. Finally, they postulated that the minimum reflux ratio of the original MFMP column corresponds to the largest minimum reflux ratio value among all decomposed simple columns. Thereafter, this assumption has been widely accepted and adopted by a number of articles, including some of the recent ones such as Caballero and Grossmann,[14] Ruiz-Marín et al.,[47] Adiche and Vogelpohl,[48] Gómez-Castro et al.,[49] Adiche and Aissa,[50] Nallasivam et al.,[18] Jiang et al.,[13,51,52] and Tumbalam Gooty et al.[19]

As we can see, in order to generalize the Underwood method to MFMP columns, existing shortcut methods incorporate several additional assumptions and constraints which cause the resulting models to only be valid under restricted settings. This work is the first to develop an accurate and easy-to-use shortcut based method to estimate the minimum reflux ratio for a general MFMP column without needing extensive simplifying assumptions. Specifically, unlike existing approaches, our method is meant to be generally applicable and does not pose any restriction on the number of feed or sidedraw streams, the relative locations and physical properties (e.g., thermal quality) of these streams, or the number of components involved in the separation. Furthermore, it is designed to be computationally efficient so that it can be incorporated into a global optimization framework. In this series, in addition to presenting how this first-of-its-kind shortcut based method is derived and formulated, we will also use our method to revisit some of the well-accepted design heuristics and modeling assumptions mentioned before. In particular, we would like to address the following key questions that distillation/separations community is concerned about:

1. What are the fundamental physical and mathematical interpretations behind the well-known Underwood method?
2. What is the optimal strategy to arrange the relative locations of feed and/or sidedraw streams in order to minimize the energy consumption. Is it always more energy efficient to place these streams based on their temperature levels?
3. Is it true that an MFMP column can always be decomposed into individual simple columns, so that its true minimum reflux ratio is given by the largest minimum reflux ratio value among all decomposed simple columns?

We will answer the first question in this article, while the remaining two will be addressed in the second article of the series. We will show that, despite widely held beliefs regarding the answers to some of the above questions, the real answers are surprising and often counterintuitive.

2 | OVERVIEW OF SOLUTION STRATEGY

We propose a bottom-up approach to solve this longstanding problem in chemical engineering. First, we recognize that the basic module or
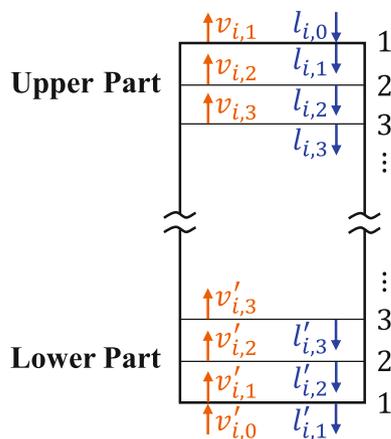
FIGURE 4 A general column section modeled as a countercurrent mass exchanger. The molar flow rate of component i in the vapor and liquid traffic leaving stage n in the lower (resp. upper) part of column section are respectively given by $v'_{i,n}$ (resp. $v_{i,n}$) and $l'_{i,n}$ (resp. $l_{i,n}$). These component flow rates are always nonnegative following the direction shown here.

building block of a general MFMP column is a column section, which can be modeled as a countercurrent mass exchange unit. As shown in Figure 3, even though the topmost and bottommost column sections in an MFMP column are respectively equivalent to the rectifying and stripping sections in a simple column, it is the presence of other intermediate column sections that really differentiates the MFMP column from a simple column. In a simple column, the net material flow of any component that is not withdrawn as a product from a column section is zero. For example, in the rectifying section of column 1 of Figure 1B, components A, B, and C have net material flows pointing upward, whereas the least volatile component D has zero net material flow. In the stripping section, components B, C, and D have net material flows pointing downward, whereas the most volatile component A has zero net material flow. However, when considering an intermediate column section in Figure 3 as highlighted by a red box, it is very likely to have some components with net material flows pointing upward and others pointing downward based on component mass balances. Due to the simultaneous presence of components with net upward and downward flows, these intermediate sections require a special mathematical treatment. Thus, rather than decomposing an MFMP column into a series of simple columns, here we construct a shortcut model for a general column section assuming ideal-VLE, CRV, and CMO as in Underwood method.[39] Also, by default, the composition, flow rate, and thermal quality of all feed and product streams are specified. These are the only assumptions we make throughout the model development. Each general column section exhibits a set of physical and mathematical properties, some of which can be interpreted geometrically and easily visualized. We will explore these properties and use them to derive the minimum reflux condition of an MFMP column as a set of algebraic constraints.

3 | MODELING COLUMN SECTION AS COUNTERCURRENT MASS EXCHANGE UNIT

We consider a general column section drawn in Figure 4 that involves a total of c components. As a result of the CMO assumption, the total vapor and liquid flow rate, respectively denoted as V and L, do not change from stage to stage within this section. The total net material upward flow $D = V - L$ stays constant as well. When the column section of interest corresponds to the topmost section of an MFMP or a simple column, D is just the total distillate flow rate. On the other hand, considering the column section to be the bottommost section of an MFMP column or the stripping section of a simple column, D is always negative and equals bottoms flow rate in magnitude. In terms of each individual component $i \in C = \{1, \cdots, c\}$, its net material upward flow rate d_i, which is given by $d_i = v'_{i,n-1} - l'_{i,n} = v_{i,n} - l_{i,n-1}$ in any stage $n \in \mathbb{N}^+$, also remains unchanged within the section. Here, $v'_{i,n}$ (resp. $v_{i,n}$) and $l'_{i,n}$ (resp. $l_{i,n}$) stand for the vapor and liquid flow rates of component i leaving stage n in the lower (resp. upper) part of column section, respectively. Notice that by convention, the component vapor ($v'_{i,n}$ or $v_{i,n}$) and liquid flows ($l'_{i,n}$ or $l_{i,n}$) are always nonnegative and follow the direction shown in Figure 4. The direction of d_i, on the contrary, is not necessarily the same for every component in the same column section. When $d_i < 0$ for some component i in the section, the net material flow direction for component i is pointing downward. Following the notations and conventions defined so far, next we will model the lower and upper part of a general column section. Subsequently, we will analyze the pinch condition in the column section as the number of stages n in both upper and lower parts approaches infinity.

In this section, our goal is to derive all relevant equations that enable calculation of stage-to-stage liquid and vapor compositions as well as potential pinch zone compositions. We first discuss the transformation of liquid component flow rates on each stage n to a new variable which encapsulates the nonlinearity associated with the ideal-VLE relation and thereby allows the solution of mass balance equations to be determined in the transformed variable space. Once the eigenvalues and eigenvectors of the transformed variable space become available, rather than immediately deriving the expressions for liquid and vapor compositions on any given stage, we take the following detour. First, we explore the connection between potential pinch zone compositions and eigenvectors in the transformed space. Next, we discuss tray-by-tray evolution of liquid composition profile in the transformed variable space. The resulting $c - 1$ dimensional pinch simplex obtained from this transformation has interesting features as each of its vertices matches exactly with a potential pinch zone liquid composition. Finally, we go back to the original problem and derive expressions for liquid and vapor compositions in the column section.

3.1 | Mass balance equations, eigenvalues, and eigenvectors

To model a general column section, we first write down the component mass balance equation:

$$
\begin{aligned}
\text{Lower part}: l'_{i,n+1} = v'_{i,n} - d_i \\
\text{Upper part}: l_{i,n} = v_{i,n+1} - d_i
\end{aligned}
\qquad \forall i \in C, n \in \mathbb{N}. \qquad (1)
$$

Note that the mass balances for the lower and upper part of a column section differ due to the way stages are numbered (see Figure 4), which is necessary especially when the column section is pinched (which implies an infinite number of stages in the section). Nevertheless, the modeling procedure is the same for both the upper and lower parts of column section. For now, we focus on the lower part to demonstrate the modeling procedure. The nonlinearity of the model originates from the ideal-VLE relation which says that, on any stage n:

$$
\frac{v'_{i,n}}{V} = \frac{\alpha_i l'_{i,n}}{\sum_{k=1}^{c} \alpha_k l'_{k,n}} \qquad \forall i \in C, n \in \mathbb{N}, \qquad (2)
$$

in which α_i stands for the relative volatility of component i with respect to the heaviest component, which is Component 1. By convention, the relative volatility of each component follows $\alpha_c > \alpha_{c-1} > \cdots > \alpha_1 = 1$. Let us consider two adjacent stages, namely $(n+1)$ and n, and substitute Equation (2) into (1):

$$
\begin{aligned}
l'_{n+1} &= \begin{pmatrix} l'_{1,n+1} \\ \vdots \\ l'_{c,n+1} \end{pmatrix} = \frac{V}{\sum_{k=1}^{c} \alpha_k l'_{k,n}} \begin{pmatrix} \alpha_1 l'_{1,n} \\ \vdots \\ \alpha_c l'_{c,n} \end{pmatrix} - \begin{pmatrix} d_1 \\ \vdots \\ d_c \end{pmatrix} \\
&= \frac{1}{\sum_{k=1}^{c} \alpha_k l'_{k,n}} \begin{pmatrix} \alpha_1(V-d_1) & -\alpha_2 d_1 & \cdots & -\alpha_c d_1 \\ -\alpha_1 d_2 & \alpha_2(V-d_2) & \cdots & -\alpha_c d_2 \\ \vdots & \vdots & \ddots & \vdots \\ -\alpha_1 d_c & -\alpha_2 d_c & \cdots & \alpha_c(V-d_c) \end{pmatrix} \begin{pmatrix} l'_{1,n} \\ l'_{2,n} \\ \vdots \\ l'_{c,n} \end{pmatrix} \\
&= \frac{1}{\boldsymbol{\alpha}^T l'_n} \left(V \mathrm{diag}(\boldsymbol{\alpha}) - \boldsymbol{d}\boldsymbol{\alpha}^T \right) l'_n,
\end{aligned} \qquad (3)
$$

where $\boldsymbol{\alpha} = (\alpha_1, \cdots, \alpha_c)^T$, $\boldsymbol{d} = (d_1, \cdots, d_c)^T$, and $\mathrm{diag}(\boldsymbol{\alpha})$ is a $c \times c$ diagonal matrix whose entries are the elements of $\boldsymbol{\alpha}$. Therefore, we can define a $c \times c$ matrix $\mathbf{A}$ as:

$$
\mathbf{A} := V \mathrm{diag}(\boldsymbol{\alpha}) - \boldsymbol{d}\boldsymbol{\alpha}^T = \begin{pmatrix} \alpha_1(V-d_1) & -\alpha_2 d_1 & \cdots & -\alpha_c d_1 \\ -\alpha_1 d_2 & \alpha_2(V-d_2) & \cdots & -\alpha_c d_2 \\ \vdots & \vdots & \ddots & \vdots \\ -\alpha_1 d_c & -\alpha_2 d_c & \cdots & \alpha_c(V-d_c) \end{pmatrix}. \qquad (4)
$$

Since $\boldsymbol{\alpha}$ and $\boldsymbol{d}$ are independent of the stage number, matrix $\mathbf{A}$ is independent of the stage number as well. Now, let us multiply both sides of Equation (3) by $\prod_{j=1}^{n-1} \boldsymbol{\alpha}^T l'_j$ and rearrange to get:

$$
l'_{n+1} \prod_{j=1}^{n} \boldsymbol{\alpha}^T l'_j = \mathbf{A} l'_n \prod_{j=1}^{n-1} \boldsymbol{\alpha}^T l'_j.
$$

Therefore, the nonlinearity associated with Equation (2) can be encapsulated by defining a new variable $\mathcal{L}'_n$ as:

$$
\mathcal{L}'_n \begin{pmatrix} \mathcal{L}'_{1,n} \\ \vdots \\ \mathcal{L}'_{c,n} \end{pmatrix} = l'_n \prod_{j=1}^{n-1} \boldsymbol{\alpha}^T l'_j \qquad \forall n \in \mathbb{N}^+, \qquad (5)
$$

from which we obtain a linear system in terms of the new variable:

$$
\mathcal{L}'_{n+1} = \mathbf{A} \mathcal{L}'_n \qquad \forall n \in \mathbb{N}^+. \qquad (6)
$$

This newly introduced variable $\mathcal{L}'_n$ not only leads to a linear system of Equation (6), but also preserves the liquid composition information and the ideal-VLE relation, as $\boldsymbol{x}'_n$, the liquid composition on stage n, and $\boldsymbol{y}'_n$, the vapor composition in equilibrium with $\boldsymbol{x}'_n$, can be determined as:

$$
\begin{aligned}
\boldsymbol{x}'_n &= \frac{l'_n}{\boldsymbol{e}^T l'_n} = \frac{\mathcal{L}'_n}{\boldsymbol{e}^T \mathcal{L}'_n} \\
\boldsymbol{y}'_n &= \frac{\mathrm{diag}(\boldsymbol{\alpha}) l'_n}{\boldsymbol{e}^T \mathrm{diag}(\boldsymbol{\alpha}) l'_n} = \frac{\mathrm{diag}(\boldsymbol{\alpha}) \mathcal{L}'_n}{\boldsymbol{e}^T \mathrm{diag}(\boldsymbol{\alpha}) \mathcal{L}'_n}
\end{aligned} \qquad \forall n \in \mathbb{N}^+. \qquad (7)
$$

Together, these two facts enable us to directly compute the composition profile in a column section without explicit tray-by-tray calculations. To show this, we first need to understand matrix $\mathbf{A}$ in Equation (4), which contains all the information about the composition profile and pinch conditions in a column section. In particular, we are interested in the fixed point solution of the linear system associated with Equation (6), which is given by the eigenvalues and eigenvectors of $\mathbf{A}$. To obtain the eigenvalues, notice that $\det(\mathbf{A} - \lambda \mathbf{I}) = \det\left[(V \mathrm{diag}(\boldsymbol{\alpha}) - \lambda \mathbf{I}) - \boldsymbol{d}\boldsymbol{\alpha}^T\right]$. Applying the matrix determinant lemma, we can determine the characteristic polynomial of $\mathbf{A}$ as:

$$
\begin{aligned}
\det(\mathbf{A} - \lambda \mathbf{I}) &= \det(V \mathrm{diag}(\boldsymbol{\alpha}) - \lambda \mathbf{I}) - \boldsymbol{\alpha}^T \mathrm{adj}(V \mathrm{diag}(\boldsymbol{\alpha}) - \lambda \mathbf{I})\boldsymbol{d} \\
&= \prod_{j=1}^{c} (V\alpha_j - \lambda) - \sum_{i=1}^{c} \alpha_i d_i \prod_{j \neq i}^{c} (V\alpha_j - \lambda) \\
&= \left(1 - \sum_{i=1}^{c} \frac{\alpha_i d_i}{V\alpha_i - \lambda}\right) \prod_{i=1}^{c} (V\alpha_i - \lambda),
\end{aligned} \qquad (8)
$$

where $\mathrm{adj}(\mathbf{M})$ stands for the adjoint of matrix $\mathbf{M}$. From Equation (8), we can easily see that the eigenvalues of $\mathbf{A}$ are:
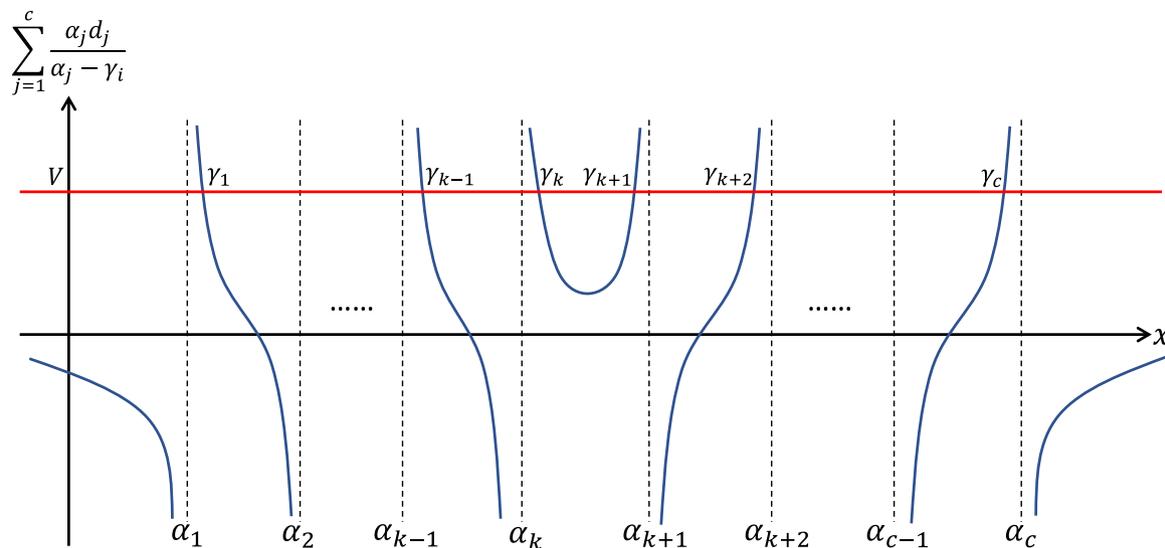
$$
\begin{aligned}
\lambda_i &= V\alpha_i \qquad \forall i \text{ such that } d_i = 0 \\
\lambda_i &= V\gamma_i \qquad \forall i \text{ such that } d_i \neq 0,
\end{aligned} \qquad (9)
$$

where γ_i represents the ith root of the following equation:

$$
\sum_{j=1}^{c} \frac{\alpha_j d_j}{\alpha_j - \gamma} = V, \qquad (10)
$$

and by convention, $\gamma_c > \cdots > \gamma_1$.

Equation (10) looks familiar. In fact, when considering the rectifying (resp. stripping) section of a simple column, this equation is identical to the Underwood distillate (resp. bottoms) equation.[40] In this

FIGURE 5 The root behavior of Equation (10) as the component net material upward flow $d_c, \cdots, d_{k+1} > 0$ and $d_k, \cdots, d_1 < 0$.

special case, we readily recognize that the Underwood roots γ_i are nothing but the eigenvalues of $\mathbf{A}$ divided by the rectifying (resp. stripping) section vapor flow V.[53] Furthermore, in this case, each Underwood root is bounded by: $\gamma_i \in (\alpha_{i-1}, \alpha_i)$ (resp. $\gamma_i \in (\alpha_i, \alpha_{i+1})$) for $i \in C$ (assuming $\alpha_0 = -\infty$ and $\alpha_{c+1} = +\infty$). For a general column section, the root behavior may be slightly different. Suppose $d_c, \cdots, d_{k+1}$ are positive and $d_k, \cdots, d_1$ are negative, Equation (10) is plotted in Figure 5. Note that there exists two distinct roots, namely γ_k and γ_{k+1}, in the interval (α_k, α_{k+1}). We will later show that these roots are indeed distinct and real when the column section has enough vapor flow V to ensure physically feasible separation in the section.

Next, for each eigenvalue λ_i determined from Equation (9), the corresponding eigenvector n_i can be obtained by standard procedure (i.e., solving $(\mathbf{A} - \lambda_i \mathbf{I})\nu_i = \mathbf{0}$) as:

$$\nu_i = \frac{1}{L}\left(\frac{\lambda_i d_1}{V\alpha_1 - \lambda_i}, \cdots, \frac{\lambda_i d_{i-1}}{V\alpha_{i-1} - \lambda_i}, \frac{\lambda_i}{\alpha_i}\left(1 - \sum_{j \neq i}^{c}\frac{\alpha_j d_j}{V\alpha_j - \lambda_i}\right),\right. \quad (11)$$

$$\left.\frac{\lambda_i d_{i+1}}{V\alpha_{i+1} - \lambda_i}, \cdots, \frac{\lambda_i d_c}{V\alpha_c - \lambda_i}\right)^T.$$

Specifically, depending on whether $d_i = 0$ or not, we have:

$$\nu_i = \frac{1}{L}\left(\frac{\alpha_i d_1}{\alpha_1 - \alpha_i}, \cdots, \frac{\alpha_i d_{i-1}}{\alpha_{i-1} - \alpha_i}, V - \sum_{j \neq i}^{c}\frac{\alpha_j d_j}{\alpha_j - \alpha_i}, \frac{\alpha_i d_{i+1}}{\alpha_{i+1} - \alpha_i},\right.$$

$$\left.\cdots, \frac{\alpha_i d_c}{\alpha_c - \alpha_i}\right)^T \quad \text{if } d_i = 0,$$

$$\nu_i = \frac{1}{L}\left(\frac{\lambda_i d_1}{V\alpha_1 - \lambda_i}, \cdots, \frac{\lambda_i d_i}{V\alpha_i - \lambda_i}, \cdots, \frac{\lambda_i d_c}{V\alpha_c - \lambda_i}\right)^T \quad (12)$$

$$= \frac{1}{L}\left(\frac{\gamma_i d_1}{\alpha_1 - \gamma_i}, \cdots, \frac{\gamma_i d_c}{\alpha_c - \gamma_i}\right)^T \quad \text{if } d_i \neq 0.$$

Since all eigenvalues will be shown to be distinct and real, these eigenvectors are linearly independent. Thus, $\mathcal{L}'_1$ can be expressed as

the linear combination of these eigenvectors, and $\mathcal{L}'_n$ can subsequently be determined by recursively applying Equation (6): $\mathcal{L}'_n = \mathbf{A}^{n-1}\mathcal{L}'_1$. Nevertheless, before going through these derivations, let us further examine the connection between eigenvector ν_i and pinch zone composition.

3.2 | Relationship between liquid pinch compositions and eigenvectors

To establish the relationship between liquid pinch zone compositions and eigenvectors of $\mathbf{A}$, recall that a pinch zone is a region in which the liquid or vapor composition remains unchanged from one stage to another. When the column section is pinched, the equilibrium curve (i.e., Equation 2) intersects the operating line (i.e., Equation 1), resulting in zero dividing force for mass transfer. The concept of pinch has been extensively discussed by Underwood[38,39] as well as Franklin and Forsyth[54] for the case of simple column operating at minimum reflux. They found that each Underwood root is related to a unique possible pinch composition. They also pointed out that, even though some of the pinch compositions calculated might not be physically feasible in an actual distillation column, they play an equally important role in constructing the composition profile inside the column section and also in deriving the minimum reflux condition. Analogously, for a general column section, each eigenvalue of Equation (9) is associated with a unique pinch composition. In fact, each ν_i exactly gives a pinch zone liquid composition associated with eigenvalue λ_i. To show this, suppose l'_{pinch} is the component liquid flow rate in the pinch zone and remains unchanged from stage to stage. Then, by Equation (3), we have $\mathbf{A}l'_{\text{pinch}} = \left(\boldsymbol{\alpha}^T l'_{\text{pinch}}\right)l'_{\text{pinch}}$, which indicates that $\boldsymbol{\alpha}^T l'_{\text{pinch}}$ must be an eigenvalue and l'_{pinch} must be an eigenvector. Thus, $l'_{\text{pinch}} = \beta\nu_i$ where β is a scalar. To determine β, for any component i with nonzero d_i, recall that $V\gamma_i = \lambda_i = \boldsymbol{\alpha}^T l'_{\text{pinch}} = \beta\boldsymbol{\alpha}^T\nu_i$, which equals to $\beta V\gamma_i/L$ from Equations (10) and (12). This implies that $\beta = L$. For any component i

with a zero d_i, $V\alpha_i = \lambda_i = \beta\boldsymbol{\alpha}^T\boldsymbol{\nu}_i$, which can be shown to equal to $\beta V\alpha_i/L$. Again, this implies that $\beta = L$. Since the argument above holds for every $i \in C$, there are as many pinch compositions as components involved in the multicomponent system. Therefore, the pinch zone component vapor and liquid flows associated with λ_i are respectively given by:

$$\boldsymbol{v}'_{\text{pinch}} = L\boldsymbol{\nu}_i + \boldsymbol{d}; \boldsymbol{l}'_{\text{pinch}} = L\boldsymbol{\nu}_i \quad \forall i \in C. \quad (13)$$

In summary, for a c-component system, there are c possible liquid pinch compositions, which are essentially the c eigenvectors $\boldsymbol{\nu}_1, \cdots, \boldsymbol{\nu}_c$. From Equations (9)–(11), all possible pinch zone liquid and vapor compositions (or pinch zone component liquid and vapor flows) will be determined once $\boldsymbol{d}$ and either V or L in the column section are known. Thus, these pinch compositions are intrinsic characteristics of a column section and are independent of which part of the column section is being considered.

3.3 | Calculation of composition profile

To calculate the composition profile within a general column section, we first diagonalize matrix $\mathbf{A}$ as $\mathbf{Q}\boldsymbol{\Lambda}\mathbf{Q}^{-1}$ using eigendecomposition, in which the columns of $\mathbf{Q}$ contain all the eigenvectors (i.e., $\mathbf{Q} = [\boldsymbol{\nu}_1, \cdots, \boldsymbol{\nu}_c]$) and $\boldsymbol{\Lambda}$ is a diagonal matrix whose diagonal elements are all the eigenvalues. To determine $\mathbf{Q}^{-1}$, we first introduce a very useful relation obtained by substituting two distinct eigenvalues, $\lambda_i = V\gamma_i$ and $\lambda_j = V\gamma_j$ (assuming $d_i, d_j \neq 0$), into Equation (10), followed by subtracting one expression from the other:

$$\sum_{k=1}^{c} \frac{\alpha_k d_k}{(\alpha_k - \gamma_i)(\alpha_k - \gamma_j)} = 0 \quad \forall i \neq j \in C. \quad (14)$$

Using Equation (14), one can verify that, for any i such that $d_i \neq 0$, the ith row of $\mathbf{Q}^{-1}$ is given by the product of a row vector ω_i^T and a scaling factor r_i that depends on λ_i:

$$\begin{aligned} \omega_i^T &= \left(\frac{V\alpha_1}{V\alpha_1 - \lambda_i}, \cdots, \frac{V\alpha_c}{V\alpha_c - \lambda_i} \right) = \left(\frac{\alpha_1}{\alpha_1 - \gamma_i}, \cdots, \frac{\alpha_c}{\alpha_c - \gamma_i} \right), \\ \frac{1}{r_i} &= \frac{V\lambda_i}{L}\sum_{k=1}^{c} \frac{\alpha_k d_k}{(V\alpha_k - \lambda_i)^2} = \frac{\gamma_i}{L}\sum_{k=1}^{c} \frac{\alpha_k d_k}{(\alpha_k - \gamma_i)^2}. \end{aligned} \quad (15)$$

It can be shown that the scaling factor r_i and d_i have the same sign. For $\lambda_i = V\alpha_i$ when $d_i = 0$, the ith row of $\mathbf{Q}^{-1}$ is simply the ith principal vector $\boldsymbol{e}_i^T$ multiplied by a scaling factor r_i:

$$\begin{aligned} \boldsymbol{w}_i^T &= \boldsymbol{e}_i^T, \\ \frac{1}{r_i} &= \frac{\lambda_i}{L\alpha_i}\left(1 - \sum_{j \neq i}^{c} \frac{\alpha_j d_j}{V\alpha_j - \lambda_i} \right) = \frac{V}{L} - \frac{1}{L}\sum_{j \neq i}^{c} \frac{\alpha_j d_j}{\alpha_j - \alpha_i}. \end{aligned} \quad (16)$$

Now that matrix $\mathbf{A}$ is diagonalized, let us now solve for the composition profile in the lower part of column section. Substituting $\mathbf{Q}\boldsymbol{\Lambda}\mathbf{Q}^{-1}$ into Equation (6), and noticing that $\mathcal{L}'_1 = \boldsymbol{l}'_1$ for the boundary case, gives $\mathcal{L}'_n = \mathbf{A}^{n-1}\mathcal{L}'_1 = \mathbf{Q}\boldsymbol{\Lambda}^{n-1}\mathbf{Q}^{-1}\boldsymbol{l}'_1$. Using Equation (7), we can

write down the liquid and vapor composition profile in the lower part of column section compactly as:

$$\begin{aligned} \boldsymbol{x}'_{n+1} &= \frac{\mathbf{Q}\boldsymbol{\Lambda}^n\mathbf{Q}^{-1}\boldsymbol{l}'_1}{\boldsymbol{e}^T\mathbf{Q}\boldsymbol{\Lambda}^n\mathbf{Q}^{-1}\boldsymbol{l}'_1} = \frac{\mathbf{Q}\boldsymbol{\Lambda}^n\mathbf{Q}^{-1}\boldsymbol{x}'_1}{\boldsymbol{e}^T\mathbf{Q}\boldsymbol{\Lambda}^n\mathbf{Q}^{-1}\boldsymbol{x}'_1} \\ \boldsymbol{y}'_n &= \frac{\text{diag}(\boldsymbol{\alpha})\mathbf{Q}\boldsymbol{\Lambda}^{n-1}\mathbf{Q}^{-1}\boldsymbol{l}'_1}{\boldsymbol{\alpha}^T\mathbf{Q}\boldsymbol{\Lambda}^{n-1}\mathbf{Q}^{-1}\boldsymbol{l}'_1} = \frac{\text{diag}(\boldsymbol{\alpha})\mathbf{Q}\boldsymbol{\Lambda}^{n-1}\mathbf{Q}^{-1}\boldsymbol{x}'_1}{(\lambda^n)^T/L\mathbf{Q}^{-1}\boldsymbol{x}'_1} \end{aligned} \quad \forall n \in \mathbb{N}, \quad (17)$$

in which we denote λ as $(\lambda_1, \cdots, \lambda_c)^T$, a column vector containing all the eigenvalues of $\mathbf{A}$. In deriving Equation (17), we apply Equations (10) and (12) and use the fact that $\boldsymbol{\alpha}^T\mathbf{Q} = \lambda^T/L$. In summary, given the set of relative volatilities ($\boldsymbol{\alpha}$), component material upward flows ($\boldsymbol{d}$), component liquid flows leaving the bottom of column section ($\boldsymbol{l}'_1$), and the total vapor flow (V), the column section composition profile can be calculated without explicit tray-by-tray calculation by first solving Equation (8) for λ_i, followed by substituting these eigenvalues to obtain $\mathbf{Q}$, $\boldsymbol{\Lambda}$, and $\mathbf{Q}^{-1}$. If we are interested in expanding the matrix representation in Equation (17), the liquid and vapor composition profiles, assuming that none of the components has a zero net material upward flow, are explicitly written as:

$$\begin{aligned} x'_{i,n+1} &= \frac{d_i}{L}\frac{\sum_{j=1}^{c}\frac{a_j\gamma_j^{n+1}}{\alpha_i - \gamma_j}}{\sum_{j=1}^{c}a_j\gamma_j^n} \\ y'_{i,n} &= \frac{\alpha_i d_i}{V}\frac{\sum_{j=1}^{c}\frac{a_j\gamma_j^n}{\alpha_i - \gamma_j}}{\sum_{j=1}^{c}a_j\gamma_j^n} \end{aligned} \quad \forall i \in C, n \in \mathbb{N},$$

where the quantity a'_j is determined to be:

$$a'_j = \frac{r_j}{L}\sum_{k=1}^{c}\frac{\alpha_k l'_{k,1}}{\alpha_k - \gamma_j} = r_j\sum_{k=1}^{c}\frac{\alpha_k x'_{k,1}}{\alpha_k - \gamma_j} \quad \forall j \in C.$$

It follows from Equation (15) that $(a'_1, \cdots, a'_c)^T = \mathbf{Q}^{-1}\boldsymbol{x}'_1$. Since $\boldsymbol{e}^T\mathbf{Q} = \boldsymbol{e}^T$ from Equation (12), we also have $\boldsymbol{e}^T\mathbf{Q}^{-1} = \boldsymbol{e}^T$ and therefore, $\sum_{j=1}^{c}a'_j = \boldsymbol{e}^T\mathbf{Q}^{-1}\boldsymbol{x}'_1 = 1$.

Similarly, when $d_i = 0$, we can show from Equation (12) that $\boldsymbol{e}^T\boldsymbol{\nu}_i = 1$. This again implies that $\boldsymbol{e}^T\mathbf{Q} = \boldsymbol{e}^T\mathbf{Q}^{-1} = \boldsymbol{e}^T$. With this, one can also write down the explicit vapor or liquid composition profile expressions for cases when some components have zero net material upward flows.

To generalize, we can define the following linear transformation that maps the original composition space in $\mathbb{R}^c$, denoted as the x-space, to a new space in $\mathbb{R}^c$, which we refer to as the z-space:

$$\boldsymbol{z}(\boldsymbol{x}) = \begin{pmatrix} z_1(\boldsymbol{x}) \\ \vdots \\ z_c(\boldsymbol{x}) \end{pmatrix} = \mathbf{Q}^{-1}\boldsymbol{x} = \begin{pmatrix} r_1\boldsymbol{w}_1^T\boldsymbol{x} \\ \vdots \\ r_c\boldsymbol{w}_c^T\boldsymbol{x} \end{pmatrix}. \quad (18)$$

By substituting Equation (18) to Equation (17), we can now express the liquid composition profile in z-space as:
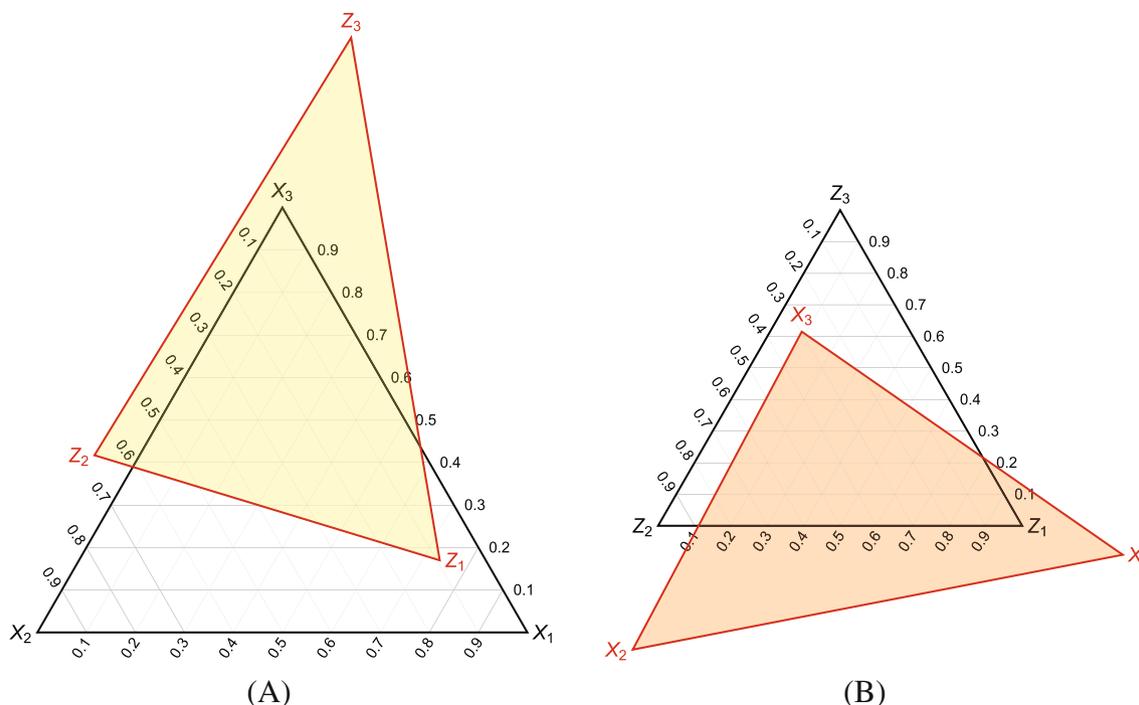
FIGURE 6 An illustrative example of composition simplex and pinch simplex drawn in x-space and z-space for $(\alpha_1, \alpha_2, \alpha_3) = (1, 1.5, 2), (d_1, d_2, d_3) = (0.03, 0.06, 0.21),$ and $V = 1.4552$. Thus, $(\gamma_1, \gamma_2, \gamma_3) = (0.9659, 1.3928, 1.7702)$ from Equation (10). (A) Composition simplex and pinch simplex in x-space; (B) Composition simplex and pinch simplex in z-space.

$$z'_{n+1} = \frac{\Lambda^n z'_1}{e^T \Lambda^n z'_1} \quad \forall n \in \mathbb{N}, \tag{19}$$

where we denote z'_1 to be $z(x'_1) = (a'_1, \cdots, a'_c)^T$ and z'_n as $z(x'_n)$. Equation (19) looks familiar. Indeed, as we will discuss shortly, it resembles the well-known Fenske equation[55] that characterizes the liquid composition profile in a simple column operated at total reflux. Such resemblance sheds light on the geometric significance of z-space.

## 3.4 | Composition profile and pinch compositions in z-space

So far, we have shown that the liquid or vapor composition profile in the lower part of a column section can be characterized either in x-space or in z-space. Specifically, the set of liquid composition profiles calculated using Equation (17) (resp. 19) with various starting compositions x'_1 (resp. z'_1) that satisfy $e^T x'_1 = 1$ (resp. $e^T z'_1 = 1$), also known as the liquid composition trajectory bundle, can be described by a $(c-1)$-dimensional simplex called the composition simplex (resp. pinch simplex). Both the composition and pinch simplices can be drawn in x-space as well as in z-space. For illustration, let us consider a ternary mixture distillation example. As shown in Figure 6A, the composition simplex drawn in x-space (C_x) is an equilateral triangle bounded by $x \geq 0$ and $e^T x = 1$. Thus, it contains all feasible compositions. The extreme points of C_x, which are denoted as $X_i = e_i$ for $i = 1, 2, 3$, correspond to the pure components in the ternary system. The facets of C_x given by $x_i = 0$ for $i = 1, 2, 3$. On the other hand,

TABLE 1 Construction of composition simplex and pinch simplex in x-space and z-space.

Composition simplex	Pinch simplex
x-space	
$C_x = \{x \in \mathbb{R}^c \mid x \geq 0, e^T x = 1\}$	$P_x = \{x \in \mathbb{R}^c \mid Q^{-1}x \geq 0, e^T x = 1\}$
Extreme points: columns of I	Extreme points: columns of Q
z-space	
$C_z = \{z \in \mathbb{R}^c \mid Qz \geq 0, e^T z = 1\}$	$P_z = \{z \in \mathbb{R}^c \mid z \geq 0, e^T z = 1\}$
Extreme points: columns of Q^{-1}	Extreme points: columns of I

the pinch simplex, P_x, is bounded by $Q^{-1}x \geq 0$ and $e^T x = 1$ in x-space. The extreme points of P_x in x-space, $Z_i = \nu_i$ for $i = 1, 2, 3$, are essentially liquid pinch compositions according to Equation (13). The facets of P_x are given by $z_i(x) = 0$ for $i = 1, 2, 3$. Of course, as shown in Figure 6B, both simplices can also be represented in the z-space. Table 1 summarizes how both simplices are constructed in both spaces.

As summarized in Table 1, when a distillation column is operated at total reflux (i.e., $d_i = 0$ for every $i \in C$), $\omega_i^T = e_i^T$ and $r_i = 1$ from Equation (16) for every $i \in C$, implying that $Q^{-1} = I$. Therefore, the pinch simplex for total reflux operation is characterized by $P_x = \{x \in \mathbb{R}^c \mid Ix \geq 0, e^T x = 1\}$, which matches with the composition simplex C_x exactly. Similarly, P_z and C_z are identical in z-space as well when the column is operated at total reflux. Furthermore, from Figure 7B, it is also clear why Equation (19) resembles the Fenske
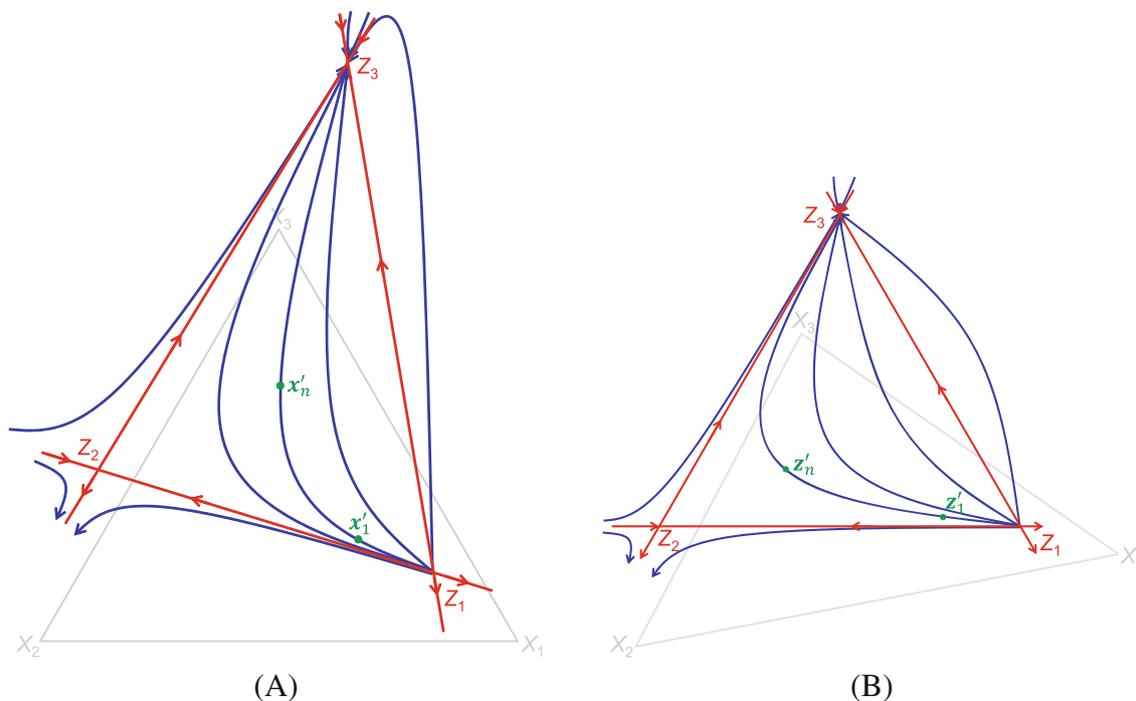
FIGURE 7 Liquid composition trajectory bundle for the illustrative example of Figure 6. The arrow indicates the direction of liquid composition evolution as we move upward from the bottom of the column section. The stage is numbered following the convention of Figure 4. (A) Liquid composition trajectory bundle drawn in x-space; (B) Liquid composition trajectory bundle drawn in z-space.

equation in z-space. Specifically, the eigenvalue matrix $\mathbf{\Lambda}$ and $\mathbf{z}'_n$ in z-space are respectively analogous to the relative volatility matrix and liquid composition $\mathbf{x}'_n$ in x-space.

An important question related to these liquid pinch compositions is: "Given the starting composition $\mathbf{x}'_1$ (or $\mathbf{z}'_1$), which pinch will be reached from the bottom of column section?" To reach a specific liquid pinch composition, say $\mathbf{Z}_i$, from the bottom of the column section, $\mathbf{Z}_i$ must first be physically feasible. From Figure 6, it can be seen that some pinch compositions ($\mathbf{Z}_2$ and $\mathbf{Z}_3$) are located outside of the feasible region bounded by the composition simplex. Suppose $d_c, \cdots, d_k > 0$ and $d_l, \cdots, d_1 < 0$ for some component $l < k$, then $\mathbf{Z}_i$ being physically feasible means that ν_i is real and nonnegative, which implies that index $i \in \{l, \cdots, k\}$ (i.e., $V\alpha_l < \lambda_i < V\alpha_k$ or $\alpha_l < \gamma_i < \alpha_k$) from Equation (11).

In addition to the requirement that $\mathbf{Z}_i$ must be physically feasible, the starting composition $\mathbf{x}'_1$ (or $\mathbf{z}'_1$) at the bottom of the column section must satisfy certain criteria in order for $\mathbf{x}'_n \to \mathbf{Z}_i$ (or ν_i) as $n \to \infty$. To see this, let us examine the liquid composition trajectory bundle drawn in Figure 7. Clearly, depending on where $\mathbf{x}'_1$ (resp. $\mathbf{z}'_1$) lies with respect to P_x (resp. P_z), the liquid composition profile follows different trajectories. From Equations (18) and (19), we can see that $\mathbf{Z}_i$ can only be reached as we move upward from the bottom of column section if the starting composition $\mathbf{x}'_1$ lies in a subspace of pinch simplex satisfying $z_j(\mathbf{x}'_1) = r_j \omega_j^T \mathbf{x}'_1 = 0$ for all $j > i$.

Before moving on, we remark that the actual pinch zone liquid composition, $\mathbf{Z}_i$, is physically feasible if and only if all c eigenvalues of matrix $\mathbf{A}$ are real. To show this, suppose $\mathbf{Z}_i$ is physically feasible, then $v'_{\text{pinch},j} = \frac{\alpha_j d_j}{\alpha_j - \gamma_i}$ is nonnegative for every component $j \in C$ from Equation (13). This implies that there is a single real root of equation $\sum_{j=1}^{c} \frac{v'_{\text{pinch},j}}{\alpha_j - x} = 0$ between α_k and α_{k+1} for every $k \in \{1, \cdots, c-1\}$.

Furthermore, comparing this equation with Equation (14), we find that these $c - 1$ distinct and real roots are essentially γ_j with $j \in C \setminus \{i\}$. On the other hand, if all eigenvalues are real, then for $\alpha_l < \gamma_i < \alpha_k$ (recall that $d_k > 0$ and $d_l < 0$), the corresponding pinch composition $\mathbf{Z}_i$ must be real and nonnegative, making it physically feasible.

3.5 | The upper part of column section

Once we successfully build the mathematical model to characterize the lower part of column section, the model for the upper part is similar. The key difference is that the numbering of stages is now reversed as indicated in Figure 4 and Equation (1). Similar to Equation (17), we can directly write down the liquid and vapor composition profile in the upper part of column section:

$$\begin{aligned} \mathbf{x}_n &= \frac{\mathbf{Q}\mathbf{\Lambda}^{-n}\mathbf{Q}^{-1}\mathbf{l}_0}{\mathbf{e}^T\mathbf{Q}\mathbf{\Lambda}^{-n}\mathbf{Q}^{-1}\mathbf{l}_0} = \frac{\mathbf{Q}\mathbf{\Lambda}^{-n}\mathbf{Q}^{-1}\mathbf{x}_0}{\mathbf{e}^T\mathbf{Q}\mathbf{\Lambda}^{-n}\mathbf{Q}^{-1}\mathbf{x}_0} \\ \mathbf{y}_{n+1} &= \frac{\text{diag}(\boldsymbol{\alpha})\mathbf{Q}\mathbf{\Lambda}^{-n-1}\mathbf{Q}^{-1}\mathbf{l}_0}{\mathbf{a}^T\mathbf{Q}\mathbf{\Lambda}^{-n-1}\mathbf{Q}^{-1}\mathbf{l}_0} = \frac{\text{diag}(\boldsymbol{\alpha})\mathbf{Q}\mathbf{\Lambda}^{-n-1}\mathbf{Q}^{-1}\mathbf{x}_0}{(\lambda^{-n})^T/L\mathbf{Q}^{-1}\mathbf{x}_0} \end{aligned} \quad \forall n \in \mathbb{N},$$

(20)

in which $\mathbf{x}_n$ can also be expressed in z-space based on the definition of Equation (18):

$$\mathbf{z}_n = \frac{\mathbf{\Lambda}^{-n}\mathbf{z}_0}{\mathbf{e}^T\mathbf{\Lambda}^{-n}\mathbf{z}_0} \quad \forall n \in \mathbb{N}, \tag{21}$$

where $\mathbf{z}_n = \mathbf{z}(\mathbf{x}_n)$. Of course, the composition and pinch simplices in x-space and z-space (Table 1) hold true irrespective of which part of column section is considered. However, the conditions for reaching a

particular pinch zone liquid composition Z_p from the top of column section as $n \to \infty$ are slightly different. This time, Z_p can be reached from the top if the starting composition x_0 lies in a subspace of pinch simplex satisfying $z_j(x_0) = r_j \omega_j^T x_0 = 0$ for all $j < p$. Clearly, a pinch zone can be reached from both the top and bottom of the column section.

To summarize, in this section, we develop a shortcut mathematical model that calculates the composition profile in a general column section without requiring explicit tray-by-tray calculations. We also derive possible pinch zone compositions and relate them with composition simplex and pinch simplex in x-space and z-space.

4 | SOME PROPERTIES OF THE MODEL

In this section, we would like to explore some of the mathematical properties of this new shortcut model, which will allow us to derive the feasible separation and minimum reflux conditions for MFMP columns.

4.1 | Existence and uniqueness of pinch zone in a general column section

Here, we would like to show that an infinite column section contains one and only one pinch zone. This is done by verifying that the same pinch zone is reached as we move into the column section from both top and bottom ends. In other words, we will show that, as n approaches infinity, v'_n and v_n converge to the same limit, which we later denote as $v = (v_1, \cdots, v_c)^T$. To illustrate the existence of pinch zone in an infinite column section, we first construct two functions $f'_n(x)$ and $f_n(x)$ for stage n in the lower and upper part of the column section, respectively:

$$
\begin{aligned}
\text{Lower part}: f'_n(x) &= \sum_{i=1}^{c} \frac{v'_{i,n}}{V\alpha_i - x}; \\
\text{Upper part}: f_n(x) &= \sum_{i=1}^{c} \frac{v_{i,n}}{V\alpha_i - x}.
\end{aligned}
\tag{22}
$$

These two functions, which have not been proposed or studied before, turn out to be quite useful. Here, we focus on the lower part of column section and explore properties for $f'_n(x)$. These properties are also valid for the upper part. Since v'_n is nonnegative on any stage n, there is a single real root $x'_k(n)$ between $V\alpha_k$ and $V\alpha_{k+1}$ for every $k \in \{1, \cdots, c-1\}$ such that $f'_n(x'_k(n)) = 0$. In fact, one can show that component vapor flow $v'_{i,n}$ is related to $x'_k(n)$ via:

$$
v'_{i,n} = V \prod_{k=1}^{c-1} \left(\alpha_i - x'_k(n)/V \right) \Big/ \prod_{\substack{k=1 \\ k \neq i}}^{c} (\alpha_i - \alpha_k) \quad \forall i \in C.
\tag{23}
$$

Furthermore, for every $k \in \{1, \cdots, c-1\}$, $x'_k(n)$ forms a monotonic sequence with respect to the stage number n:

Proposition 1. *The roots of $f'_n(x) = 0$ form a monotonic sequence $\{x'_k(n)\}$ with respect to n for every $k \in \{1, \cdots, c-1\}$.*

Proof. We take the fractional part of the characteristic polynomial of A and define a function $C(x)$ as:

$$
C(x) := \sum_{i=1}^{c} \frac{\alpha_i d_i}{V\alpha_i - x} - 1,
\tag{24}
$$

and observe that $C(x)$ is independent of stage number n. Substituting the mass balance equation $v'_n - l'_{n+1} = d$, the ideal-VLE relation $l'_n L = \frac{\text{diag}(1/\alpha)v'_n}{e^T \text{diag}(1/\alpha)v'_n}$, and $e^T y_n = 1$ into Equation (24), we obtain $C(x) = \frac{1}{V}\left[x f'_n(x) - \alpha^T l'_{n+1} f'_{n+1}(x) \right]$. Thus, $C(x'_k(n)) = -\alpha^T l'_{n+1} f'_{n+1}(x'_k(n)) = \frac{x'_k(n)}{V} f'_{n-1}(x'_k(n))$, implying $f'_{n+1}(x'_k(n)) \cdot f'_{n-1}(x'_k(n)) \leq 0$. Since $v'_n \geq 0$, $f'_n(x)$ monotonically increases with x between $V\alpha_k$ and $V\alpha_{k+1}$. Therefore, $x'_k(n)$ lies within $x'_k(n-1)$ and $x'_k(n+1)$. If $x'_k(n+1) \geq x'_k(n-1)$, $\{x'_k(n)\}$ is a monotonically increasing sequence. Otherwise, it is monotonically decreasing. In either case, $\{x'_k(n)\}$ is monotonic. □

Since $\{x'_k(n)\}$ is bounded and monotonic, it is a convergent sequence. Let us denote $x'_k(n) \to x'_k$ as $n \to \infty$ for every $k \in \{1, \cdots, c-1\}$. Figure 8 shows convergence of sequence $\{x'_k(n)\}$ for the lower part of the rectifying section of a simple column simulated in Aspen HYSYS V11 using actual column vapor composition profile data. Note that it follows from Equation (23) and Figure 8 that $v'_{k,n} \to 0$ when and only when $x'_k(n) \to V\alpha_k$ (i.e., $x'_k = V\alpha_k$). In other cases when $v'_{k,n} \not\to 0$, it can be shown that $x'_k(n)$ is bounded away from both $V\alpha_k$ and $V\alpha_{k+1}$. We can also bound $\frac{df'_n(x)}{dx}$ at the root $x'_k(n)$ in a stage-independent manner. Specifically, $\frac{df'_n(x)}{dx} = \sum_{i=1}^{c} \frac{v_{i,n}}{(V\alpha_i - x)^2}$, whose denominator is bounded away from zero at $x'_k(n)$. Therefore, $\frac{df'_n(x)}{dx}$ can be upper bounded by V/δ^2, where $0 < \delta \leq \min\{x - V\alpha_k, V\alpha_{k+1} - x\}$. A valid lower bound for $\frac{df'_n(x)}{dx}$ is zero. Using these bounds, for $\lim_{n\to\infty} v'_{k,n} \neq 0$, we can show that $C(x'_k(n)) \to 0$ as $n \to \infty$:

Proposition 2. $\{C(x'_k(n))\}$ *is a convergent sequence and $C(x'_k) = 0$ when $\lim_{n\to\infty} v'_{k,n} \neq 0$.*

Proof. Recall that $C(x'_k(n)) = -\frac{L}{\sum_{j=1}^{c} v'_{j,n+1}/\alpha_j} f'_{n+1}(x'_k(n))$ and note that the term $\frac{L}{\sum_{j=1}^{c} v'_{j,n+1}/\alpha_j}$ can be lower bounded by $\frac{L\alpha_1}{V}$. According to the mean value theorem, for $x'_k(n)$ sufficiently close to $x'_k(n+1)$:

$$
0 \leq C(x'_k(n)) \leq \frac{L\alpha_1}{V}\left[f'_{n+1}(x'_k(n+1)) - f'_{n+1}(x'_k(n)) \right]
$$
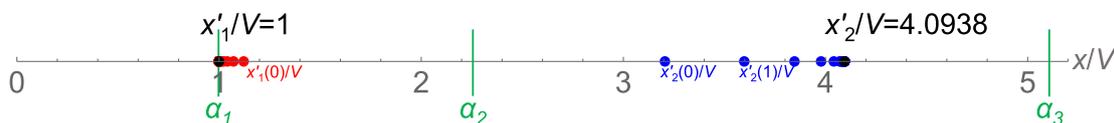
FIGURE 8 Convergence of monotonically decreasing sequence $\{x_1'(n)\}$ and monotonically increasing sequence $\{x_2'(n)\}$ for the rectifying section of a simple column separating an equimolar saturated liquid feed of n-octane (Component 1), n-heptane (Component 2), and n-hexane (Component 3), where $(\alpha_1, \alpha_2, \alpha_3) = (1, 2.2500, 5.1168)$. The reflux ratio is set to be 2.0, and the distillate flow rate is half of the feed flow rate and contains 66.67 mol% n-hexane and 33.33 mol% n-heptane.

$$\leq \frac{L\alpha_1}{V}\frac{V}{\delta^2}\left\|x_k'(n+1)-x_k'(n)\right\|$$

$$= \frac{L}{\delta^2}\left\|x_k'(n+1)-x_k'(n)\right\|.$$

Since $\left\|x_k'(n+1)-x_k'(n)\right\| \to 0$ as $n \to \infty$, it follows from the continuity of $C(x)$ within $x \in (V\alpha_k, V\alpha_{k+1})$ that $\lim_{n\to\infty} C(x_k'(n)) = C(x_k') = 0$. $\qquad\square$

Summarizing the findings above, especially from Equation (23) and Propositions 1 and 2, we conclude that, with component vapor flows always staying nonnegative, v_n' eventually converges to a limit denoted as $v' = \lim_{n\to\infty} v_n' = (v_1', ..., v_c')^T$. Similarly, component liquid flow l_n' also converges to a limit $l' = v' - d \geq 0$. In other words, a pinch zone forms in an infinite column section. Let the limiting function of the sequence $\left\{f_n'(x)\right\}$ be $f(x)\sum_{i=1}^{c}\frac{v_i'}{V\alpha_i - x}$, which also has $c-1$ distinct real roots, namely $x_1' < x_2' < \cdots < x_{c-1}'$ with $x_k' \in [V\alpha_k, V\alpha_{k+1}]$. Inside the pinch zone, $f_n'(x) = f_{n+1}'(x) = f(x)$, and thus $C(x) = \frac{1}{V}\left(x - \boldsymbol{\alpha}^T l'\right)f(x)$. Note that the roots of $C(x) = 0$, which are $x_1', \cdots, x_{c-1}', \boldsymbol{\alpha}^T l'$, are solutions of a c-degree polynomial with real coefficients. Therefore, if complex roots exist, there must be at least two of them forming complex conjugate. However, since all $c-1$ roots of $f(x) = 0$ are distinct and real, it follows that all roots of $C(x) = 0$ must be real in pinch zone as $n \to \infty$. Furthermore, these roots are consistent with the eigenvalues of $\mathbf{A}$ determined from its characteristic polynomial. Therefore, although we do not yet have a rigorous proof, given $d_c, \cdots, d_k > 0$, $d_{k-1}, \cdots, d_{l+1} = 0$, and $d_l, \cdots, d_1 < 0$ for some $l < k$ in a column section, based on Equation (9), Figure 5, as well as numerical simulation results obtained from numerous case studies, we have sufficient evidence and confidence to relate all roots of $f(x) = 0$ with $c-1$ of the c roots of $C(x) = 0$:

$$\begin{aligned} x_i' &= \lambda_i = V\gamma_i \in (V\alpha_i, V\alpha_{i+1}) & \text{for } i \in \{1, \cdots, l\} \\ x_i' &= \lambda_i = V\alpha_i & \text{for } i \in \{l+1, \cdots, k-1\} \\ x_i' &= \lambda_{i+1} = V\gamma_{i+1} \in (V\alpha_i, V\alpha_{i+1}) & \text{for } i \in \{k, \cdots, c-1\}. \end{aligned} \tag{25}$$

The remaining root of $C(x) = 0$, $\boldsymbol{\alpha}^T l'$, corresponds to the remaining eigenvalue of $\mathbf{A}$ denoted as λ_p. It turns out that $\boldsymbol{\alpha}^T l'$ or λ_p is closely related to the actual pinch zone composition and therefore will be referred to as the pinch root or pinch eigenvalue. For the boundary cases, when $d_i < 0$ for all $i \in C$, which is the case in the bottommost section of an MFMP column, we set $l = c-1$ and $k = c$ so that

Equation (25) simply becomes $x_i' = \lambda_i = V\gamma_i \in (V\alpha_i, V\alpha_{i+1})$ for $i \in \{1, \cdots, c-1\}$. In this case, $\lambda_p = \lambda_c = V\gamma_c > V\alpha_c$. When $d_i > 0$ for all $i \in C$, which is the case in the topmost section of an MFMP column, we set $l = 0$ and $k = 1$ and Equation (25) simply reduces to $x_i' = \lambda_{i+1} = V\lambda_{i+1} \in (V\alpha_i, V\alpha_{i+1})$ for $i \in \{1, \cdots, c-1\}$. And in this case, $\lambda_p = \lambda_1 = V\gamma_1 < V\alpha_1 = V$. On the other hand, when $1 \leq l < k \leq c-1$, it can be shown from Equation (25) that $\lambda_p = \lambda_k \in (V\alpha_{k-1}, V\alpha_k) \subset (V\alpha_l, V\alpha_k)$.

Since there is only one set of eigenvalues $\lambda_1, \cdots, \lambda_c$ for a particular column section, the solutions to the limiting function for the sequence $\{f_n(x)\}$ characterizing the upper part of column section are identical to the solutions of $C(x) = 0$ for the lower part. Therefore, from Equation (23), both the upper and lower parts converge to the same pinch zone as $n \to \infty$ from both ends. The component vapor and liquid flows in this unique pinch zone are denoted as $v = v'$ and $l = l'$, respectively. This means that $\boldsymbol{\alpha}^T l = \boldsymbol{\alpha}^T(v - d) = \lambda_p$, which can be rearranged to get:

$$\begin{aligned} v &= \left(\frac{V\alpha_1 d_1}{V\alpha_1 - \lambda_p}, ..., \frac{V\alpha_c d_c}{V\alpha_c - \gamma_p}\right)^T = \omega_p \circ d; \quad l = \left(\frac{\lambda_p d_1}{V\alpha_1 - \lambda_p}, ..., \frac{\lambda_p d_c}{V\alpha_c - \lambda_p}\right)^T \\ &= L\nu_p, \end{aligned} \tag{26}$$

where the symbol $\circ$ stands for the Hadamard product. Comparing Equations (13) and (26) implies that the actual pinch zone liquid composition is Z_p. Recall from the previous section that for $d_c, \cdots, d_k > 0$ and $d_l, \cdots, d_1 < 0$ for some $l < k$ in an infinite column section, pinch Z_p is physically feasible if and only if $V\alpha_l < \lambda_p < V\alpha_k$. In other words, the pinch eigenvalue must lie in the interval where the sign change in component net upward flow occurs. Furthermore, since a single pinch zone is reached from the top and bottom of an infinite column section, we remark that at most one sign change in the elements of d is allowed for a physically feasible pinch zone to develop in an infinite column section.

4.2 | Relating eigenvalues to the inlet stream compositions in an infinite column section

Now we would like to study how the liquid (l_0) and vapor streams (v_0') entering an infinite column section (see Figure 4) are related to the eigenvalues of $\mathbf{A}$, provided that the pinch zone is Z_p. We are interested in understanding this connection because l_0 and v_0' come from neighboring column sections as leaving streams. Thus, by building

connections between the eigenvalues that characterize the internal flow behavior of the column section of interest and boundary component liquid and vapor flows, we can uncover relations that need to be satisfied as different column sections are stacked back to form the original MFMP column. To start, we define two functions $F_1(x)$ and $F_2(x)$ as follows:

$$F_1(x) = \sum_{i=1}^{c} \frac{\alpha_i v'_{i,0}}{V\alpha_i - x} - 1, \qquad (27)$$

$$F_2(x) = \sum_{i=1}^{c} \frac{\alpha_i l_{i,0}}{V\alpha_i - x}. \qquad (28)$$

It can be shown that $F_1(x) = \frac{x}{V}f'_0(x) = \frac{\alpha^T l'_1}{V}f'_1(x) + C(x)$, and $F_2(x)$ can be rewritten as $\frac{x}{V}f_1(x) - C(x)$. The roots of $F_1(x) = 0$ and $F_2(x) = 0$ are denoted as $0 = \varphi_0 < \varphi_1 < \cdots < \varphi_{c-1}$ and $\phi_1 < \cdots < \phi_{c-1}$, respectively. Clearly, φ_k and ϕ_k roots lie in the interval between $V\alpha_k$ and $V\alpha_{k+1}$ for $k \in \{1, \cdots, c-1\}$. These roots are related to the eigenvalues of $\mathbf{A}$.

Proposition 3. *The eigenvalues of $\mathbf{A}$ are related to the roots of $F_1(x) = 0$ and $F_2(x) = 0$ as follows:*

$$\lambda_i = \varphi_{i-1} \qquad \forall \lambda_i > \lambda_p;$$

$$\lambda_i = \phi_i \qquad \forall \lambda_i < \lambda_p.$$

Proof. $f'_n(\lambda_i)$ in Equation (22) can be compactly written as $f'_n(\lambda_i) = \omega_i^T \text{diag}(V\alpha)^{-1} v'_n$. We substitute Equation (17) into this compact form and get:

$$f'_0(\lambda_i) = \frac{\omega_i^T \mathbf{Q}\Lambda^{-1}\mathbf{Q}^{-1}\mathbf{x}'_1}{e^T \mathbf{Q}^{-1}\mathbf{x}'_1} = (\omega_i^T \nu_1, \cdots, \omega_i^T \nu_c)\Lambda^{-1}\mathbf{z}'_1,$$

where we use $e^T \mathbf{Q}^{-1} = e^T$. Recall from Equation (14) and the definition of $\mathbf{Q}$ and $\mathbf{Q}^{-1}$ that $\omega_i^T \nu_j$ is 0 for any $j \in C \setminus \{i\}$ and equals $1/r_i$ if and only if $i = j \in C$, which implies that $f'_0(\lambda_i) = \left(0, \cdots, 0, \frac{1}{\lambda_i r_i}, 0, \cdots, 0\right)\mathbf{z}'_1 = \frac{z_i(\mathbf{x}'_1)}{\lambda_i r_i} = \frac{1}{\lambda_i}\omega_i^T \mathbf{x}'_1$. So $F_1(\lambda_i) = \frac{\lambda_i}{V}f'_0(\lambda_i) = \omega_i^T \mathbf{x}'_1/V$. Since the actual pinch zone liquid composition is $\mathbf{Z}_p$, $\omega_i^T \mathbf{x}'_1 = 0$ for all $i > p$, because otherwise the eigenvector with a larger eigenvalue would survive with repeated applications of Equation (6). This means $\lambda_i = \varphi_{i-1} \in [V\alpha_{i-1}, V\alpha_i]$ for every $\lambda_i > \lambda_p$. $\qquad \square$

Similarly, $f_n(\lambda_i)$ in Equation (22) can be written as $f_n(\lambda_i) = \omega_i^T \text{diag}(V\alpha)^{-1}v_n$. Substituting Equations (20) and (14) yields $f_1(\lambda_i) = \omega_i^T \mathbf{Q}\Lambda^{-1}\mathbf{Q}^{-1}\mathbf{x}_0 = \left(0, \cdots, 0, \frac{1}{\lambda_i r_i}, 0, \cdots, 0\right)\mathbf{z}_0 = \frac{1}{\lambda_i}\omega_i^T \mathbf{x}_0$. So $F_2(\lambda_i) = \omega_i^T \mathbf{x}_0/V - C(\lambda_i) = \omega_i^T \mathbf{x}_0$. Again, since $\mathbf{Z}_p$ is the actual pinch zone liquid composition, $F_2(\lambda_i) = 0$ for all $i < p$. In other words, $\lambda_i = \phi_i \in [V\alpha_i, V\alpha_{i+1}]$ for every $\lambda_i < \lambda_p$.

Proposition 3 tells us that, on any stage in the lower part of column section (i.e., between the pinch zone $\mathbf{Z}_p$ and the bottom of column section), all eigenvalues larger than the pinch eigenvalue λ_p are

also roots of $f'_n(x) = 0$. Meanwhile, as we move infinitely up from the bottom of column section into the pinch zone, all roots of $f'_n(x)$ eventually match with all the eigenvalues (or roots of $C(x) = 0$) besides λ_p as $C(x) = (x - \lambda_p)f(x)$. Together with Proposition 1, we see that as n increases, the roots of $f'_n(x) = 0$ that are smaller than λ_p will move monotonically toward and eventually converge to $\lambda_i < \lambda_p$, which can also be obtained from the roots of $F_2(x) = 0$ (see Figure 9B). Similarly, on any stage in the upper part of column section, all eigenvalues smaller than λ_p are also roots of $f_n(x) = 0$. As we move infinitely down from the top of column section to the pinch zone, roots of $f_n(x) = 0$ eventually become the same as all the roots of $C(x) = 0$ except for λ_p. Thus, as n increases, the roots of $f_n(x) = 0$ larger than λ_p move monotonically toward all $\lambda_i > \lambda_p$, which can also be obtained from the roots of $F_1(x) = 0$ (see Figure 9C).

In other words, once v'_0 and l_0 are known, we can track the movement of eigenvalues as n increases in both directions except the pinch eigenvalue λ_p. For λ_p, without loss of generality, suppose that $d_c, \cdots, d_{k+1} > 0$ and $d_k, \cdots, d_1 < 0$ in a column section. In this case, we know that λ_p must lie in $(V\alpha_k, V\alpha_{k+1})$. On top of this, we can impose a tighter bound on λ_p, as illustrated in Proposition 4 below.

Proposition 4. *If the pinch eigenvalue λ_p (or root of $C(x) = 0$) lies in $(V\alpha_k, V\alpha_{k+1})$, then it is further bounded away from $[\min\{\phi_k, \varphi_k\}, \max\{\phi_k, \varphi_k\}]$.*

Proof. We know that there are two roots of $C(x) = 0$ in $(V\alpha_k, V\alpha_{k+1})$. When λ_p is the larger root, let the other root of $C(x) = 0$ be denoted as λ_{p-1}. From Proposition 3, $\phi_k = \lambda_{p-1} < \lambda_p$. To show that $\lambda_p > \varphi_k$, we only need to show the case when $\phi_k < \varphi_k$, as the other case is trivially satisfied. When $\phi_k < \varphi_k$, recall from Proposition 3 that $\phi_k = x'_k$ and $\varphi_k = x'_k(0)$ as $F_1(x) = \frac{x}{V}f'_0(x)$, implying that $F_1(x) = 0$ shares roots with $f'_0(x) = 0$. Since $x'_k < x'_k(0)$, by Proposition 1, $\{x'_k(n)\}$ is a monotonically decreasing sequence, and thus $f'_1(\varphi_k) = f'_1(x'_k(0)) > f'_1(x'_k(1)) = 0$. Since $F_1(x)$ can also be expressed as $\frac{\alpha^T l'_1}{V}f'_1(x) + C(x)$, $C(\varphi_k) = -\frac{\alpha^T l'_1}{V}f'_1(\varphi_k) < 0$. Thus, $\lambda_{p-1} < \varphi_k < \lambda_p$, or $\lambda_p > \max\{\phi_k, \varphi_k\}$. When λ_p is the smaller root of $C(x) = 0$ in $(V\alpha_k, V\alpha_{k+1})$, let the other root be denoted as λ_{p+1}. From Proposition 3, $\lambda_p < \lambda_{p+1} = \varphi_k$. We now show that $\lambda_p < \phi_k$ as well. The statement is obvious if $\phi_k > \varphi_k$. If $\phi_k < \varphi_k$, $\{x_k(n)\}$ is a monotonically increasing sequence. Thus, $f_1(x_k(1)) = 0 > f_1(x_k(0)) = f_1(\phi_k)$. Since $F_2(\phi_k) = \frac{\phi_k}{V}f_1(\phi_k) - C(\phi_k) = 0$, $C(\phi_k) < 0 = C(\lambda_p)$. Thus, $\lambda_p < \phi_k < \lambda_{p+1}$, or $\lambda_p < \min\{\phi_k, \varphi_k\}$. $\qquad \square$

Proposition 4 is also highlighted in Figure 9B. Essentially, in an infinite column section with $\mathbf{Z}_p$ as the pinch, all eigenvalues of $\mathbf{A}$ (or all roots of $C(x) = 0$), $\lambda_1, \cdots, \lambda_c$, are determined once the streams entering the column section from top and bottom are known. Propositions 1 through 4 state that l_0 determines all $\lambda_i < \lambda_p$, whereas v'_0 determines all $\lambda_i > \lambda_p$. And the pinch root λ_p is more tightly bounded.
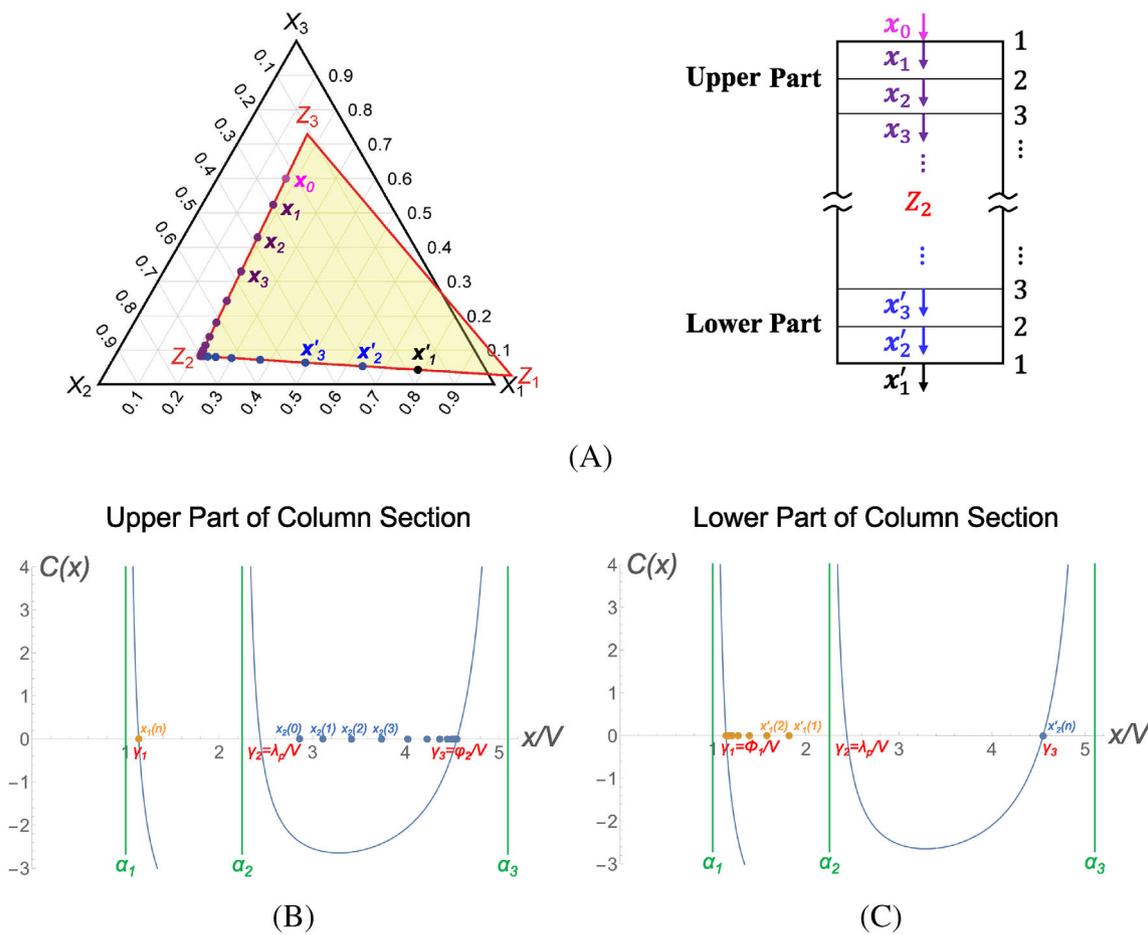
FIGURE 9 In this example, we consider an infinite column section separating n-octane (Component 1), n-heptane (Component 2), and n-hexane (Component 3), with $(\alpha_1, \alpha_2, \alpha_3) = (1, 2.2500, 5.1168)$, $(d_1, d_2, d_3) = (-0.7, -0.3, 0.5)$, and $V = 5$. (A) The pinch simplex and liquid composition profile for this column section. When the liquid pinch composition is Z_2, the pinch eigenvalue $\lambda_p = \lambda_2 \in (V\alpha_2, V\alpha_3)$. The liquid stream leaving (resp. entering) the column section from the bottom (resp. top) has a composition of x'_1 (resp. x_0). The liquid compositions in the lower (resp. upper) part of column section satisfy $z_3(x'_n) = 0$ (resp. $z_1(x_n) = 0$), which leads to $\lambda_3 = \varphi_2$ (resp. $\lambda_1 = \phi_1$); (B) Movement of $x_k(n)$ roots of $f_n(x) = 0$ for the upper part of column section. It is clear that $\lambda_2 < \min\{\phi_2, \varphi_2\}$ for the upper part of column section; (C) Movement of $f'_n(x)$ for the lower part.

5 | STACKING OF ADJACENT COLUMN SECTIONS

Up to this point, we have been focusing on modeling and understanding a single column section, which is the basic module for an MFMP column. Next, we will stack back and connect these individual sections to form the original MFMP column through liquid and vapor balances. Figure 10 presents a generalized illustration of how adjacent sections are linked by a feed or sidedraw stream. Specifically, when a feed stream F is introduced to the column, its vapor portion directly enters section TOP$_F$ together with the vapor stream coming from the top stage of section BOT$_F$. The liquid portion of the feed is mixed with the liquid coming from the bottom downcomer of section TOP$_F$. We would like to remark that such a feed arrangement differs slightly from the one used by Underwood[38,39] as well as Acrivos and Amundson,[53] where the feed stream enters the column onto a "feed stage" that does not belong to either TOP$_F$ or BOT$_F$. In the "feed

stage" model, the feed stream is perfectly mixed with the incoming liquid and vapor streams on the feed stage, and the liquid and vapor streams leaving the feed stage are in complete thermodynamic equilibrium with each other. Despite such differences, Kolokolnikov et al.[56] showed that both feed arrangements would lead to the same results in minimum reflux requirement for the case of a simple column. And relying on Kolokolnikov et al.'s argument, we will split the feed flow into vapor and liquid portions as described above to introduce a feed stream into two general column sections stacked on one another. Furthermore, compared to the "feed stage" model, our model more realistically captures how a feed stream interacts with internal liquid and vapor traffic in an actual column, as it avoids the potential flooding issue.[57] When it comes to sidedraw stream W, the vapor portion is directly withdrawn as part of the vapor stream from BOT$_W$, whereas the liquid portion is taken out from the liquid stream from TOP$_W$ by means of downcomer trapout or chimney tray.[57] Also, it is worth noting that, when we label a column section as
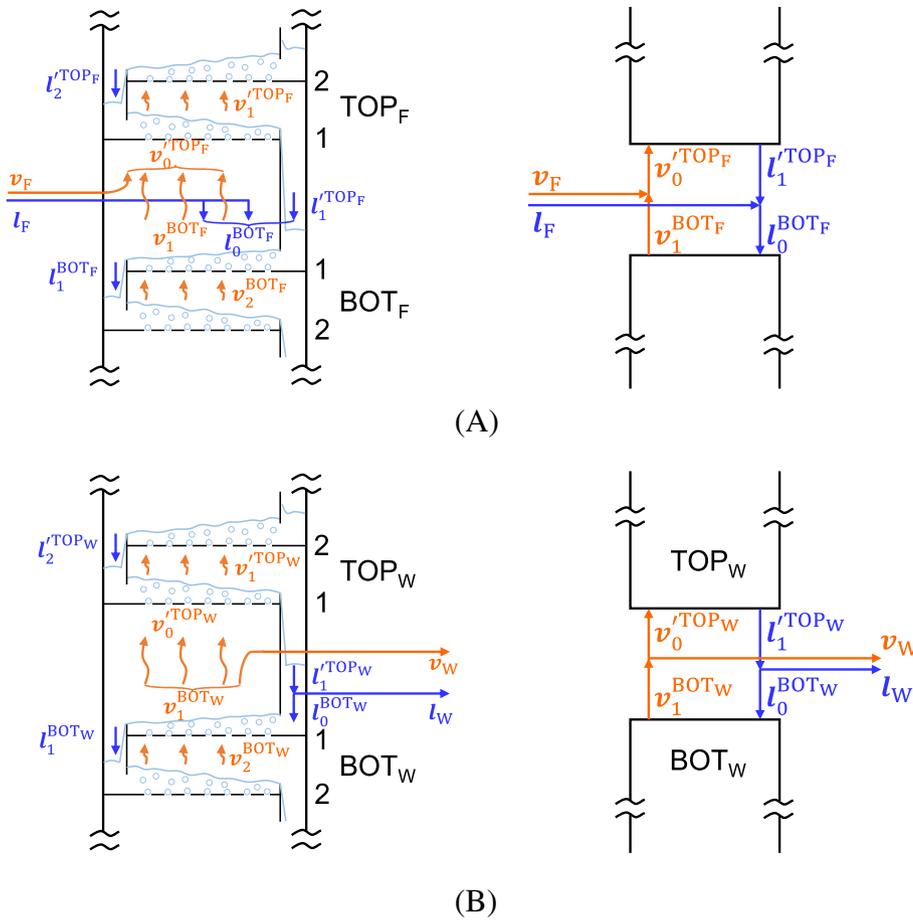
FIGURE 10 Two column sections connected by (A) a feed stream and (B) a sidedraw stream. Note that $v_0^{'TOP_F}$ and $l_0^{BOT_F}$ are generally not in equilibrium with each other. As shown in (A), in the presence of a two-phase feed stream, l_F and v_F are in equilibrium. For sidedraw W, v_W, $v_1^{BOT_W}$, and $v_0^{'TOP_W}$ all have the same composition, so do l_W, $l_1^{TOP_W}$, and $l_0^{BOT_W}$.

either the "top" or "bottom" section, such labeling is with respect to the specific feed or sidedraw stream being considered. For example, in the two-feed, three-product column drawn in Figure 2, column Section 3 can be viewed as the top section with respect to feed stream BCD or the bottom section with respect to sidedraw stream BC.

Under the simplifying assumption that these components form an ideal mixture, and assuming that complete thermodynamic equilibrium is achieved on every stage, we have the following liquid and vapor balance equations around the feed or sidedraw stream:

For feed F:
$$v_1^{BOT_F} + v_F = v_0^{'TOP_F} \quad l_1^{'TOP_F} + l_F = l_0^{BOT_F} \quad v_F + l_F = f_F$$
$$v_0^{'TOP_F} - l_1^{'TOP_F} = d^{TOP_F} \quad v_1^{BOT_F} - l_0^{BOT_F} = d^{BOT_F},$$

For sidedraw W:
$$v_0^{'TOP_W} + v_W = v_1^{BOT_W} \quad l_0^{BOT_W} + l_W = l_1^{'TOP_W} \quad v_W + l_W = f_W$$
$$v_0^{'TOP_W} - l_1^{'TOP_W} = d^{TOP_W} \quad v_1^{BOT_W} - l_0^{BOT_W} = d^{BOT_W}.$$

(29)

5.1 | Identifying eigenvalue relationships for adjacent column sections connected by a feed stream

When two column sections are connected by a feed stream, depending on the value of section vapor flow V^{TOP_F} (or V^{BOT_F}), exactly one of the following three scenarios will occur:

1. Column sections are pinched, in which case the target separation goal can only be achieved with an infinite number of stages.
2. Target separation can be achieved in the column sections using a finite number of stages.
3. Target separation cannot be achieved even with an infinite number of stages.

Note that only the first two scenarios indicate that the target separation goal is feasible in the column sections considered. Next, we will derive conditions describing each of the scenarios, from which algebraic constraints for a feasible separation in an MFMP column can be obtained. Note that the minimum reflux operation is simply the extreme case of feasible separation in the column. We will also provide geometric interpretations of these algebraic constraints in terms of pinch simplex.

In Scenario 1, since the column sections are pinched, let us denote the actual pinch zone liquid compositions in TOP_F and BOT_F as $Z_p^{TOP_F}$ and $Z_p^{BOT_F}$, respectively. The corresponding pinch eigenvalues are denoted as $\lambda_p^{TOP_F}$ and $\lambda_p^{BOT_F}$, respectively. Clearly, since a feed stream introduces materials into the column, $d^{TOP_F} - d^{BOT_F} = v_F + l_F > 0$, which implies that the indices of pinch eigenvalues satisfy $p^{TOP_F} \leq p^{BOT_F}$. In addition, Proposition 3 states that $F_1^{TOP_F}\left(\lambda_i^{TOP_F}\right) = 0$ for every $\lambda_i^{TOP_F} V^{TOP_F} \in [\alpha_{i-1}, \alpha_i]$ that is greater than $\lambda_p^{TOP_F} V^{TOP_F}$, and

$F_2^{BOT_F}\left(\lambda_i^{BOT_F}\right)=0$ for every $\lambda_i^{BOT_F}V^{BOT_F}\in[\alpha_i,\alpha_{i+1}]$ that is less than $\lambda_p^{BOT_F}V^{BOT_F}$. Therefore, we can define an index set I_F as:

$$I_F=\left\{i\in C|\lambda_i^{TOP_F}>\lambda_p^{TOP_F},\lambda_{i-1}^{BOT_F}<\lambda_p^{BOT_F}\right\}=\left\{p^{TOP_F}+1,\cdots,p^{BOT_F}\right\},\quad(30)$$

with $d_i^{TOP_F}>0$ and $d_{i-1}^{BOT_F}<0$ simultaneously satisfied for all $i\in I_F$. For example, consider a five-component system. Suppose $d_1^{TOP_F}<0$ and $d_2^{TOP_F},\cdots,d_5^{TOP_F}>0$, whereas $d_1^{BOT_F},\cdots,d_3^{BOT_F}<0$ and $d_4^{BOT_F},d_5^{BOT_F}>0$. From Equation (25), the pinch index $p^{TOP_F}=2$ and $p^{BOT_F}=4$. Thus, $\lambda_3^{TOP_F},\lambda_4^{TOP_F},\lambda_5^{TOP_F}>\lambda_p^{TOP_F}$, and $\lambda_1^{BOT_F},\lambda_2^{BOT_F},\lambda_3^{BOT_F}<\lambda_p^{BOT_F}$. And the index set $I_F=\{3,4\}$.

Once this index set is defined, let us consider the general case in which feed F is a two-phase stream. Given $l_F>0$, $v_F>0$, and d^{TOP_F}, we can first determine the section vapor flow V^{TOP_F} that will enable roots $\gamma_i^{TOP_F}$ obtained from Equation (10) to satisfy:

$$\sum_{j=1}^{c}\frac{\alpha_j l_{j,F}}{\alpha_j-\gamma_i^{TOP_F}}=0,\quad(31)$$

for all $i\in I_F$. In other words, when section TOP_F has this specific vapor flow V^{TOP_F}, the pinch simplex for section TOP_F satisfies $z_i^{TOP_F}(l_F)=0$ from Equation (18) for all $i\in I_F$.

Also, since v_F and l_F are in thermodynamic equilibrium, $\sum_{j=1}^{c}\frac{v_{j,F}}{\alpha_j-\gamma_i^{TOP_F}}=0$ for every $i\in I_F$ due to Equation (2). This leads to two additional relationships for these $\gamma_i^{TOP_F}$ roots for all $i\in I_F$ use this particular vapor flow V^{TOP_F}:

$$\begin{aligned}\sum_{j=1}^{c}\frac{\alpha_j v_{j,F}}{\alpha_j-\gamma_i^{TOP_F}}&=\sum_{j=1}^{c}\frac{\left(\alpha_j-\gamma_i^{TOP_F}\right)v_{j,F}+\gamma_i^{TOP_F}\cdot v_{j,F}}{\alpha_j-\gamma_i^{TOP_F}}=V_F+0=V_F,\\\sum_{j=1}^{c}\frac{\alpha_j f_{j,F}}{\alpha_j-\gamma_i^{TOP_F}}&=\sum_{j=1}^{c}\frac{\alpha_j\left(l_{j,F}+v_{j,F}\right)}{\alpha_j-\gamma_i^{TOP_F}}=V_F.\end{aligned}\quad(32)$$

Now, substituting Equations (31) and (32) into Equations (10) and (29), we can see that $V^{TOP_F}-V_F=V^{BOT_F}=\sum_{j=1}^{c}\frac{\alpha_j\left(d_j^{TOP_F}-f_{j,F}\right)}{\alpha_j-\gamma_i^{TOP_F}}=\sum_{j=1}^{c}\frac{\alpha_j d_j^{BOT_F}}{\alpha_j-\gamma_i^{TOP_F}}$ for every $i\in I_F$. This implies that roots $\gamma_i^{TOP_F}$ actually match with roots $\gamma_{i-1}^{BOT_F}$ for $i\in I_F$ for this particular section vapor flow, as both $\gamma_i^{TOP_F}$ and $\gamma_{i-1}^{BOT_F}$ lie in the same interval $[\alpha_{i-1},\alpha_i]$. Let us denote this set of common roots as $\rho_{i-1,F}=\gamma_i^{TOP_F}=\gamma_{i-1}^{BOT_F}\in[\alpha_{i-1},\alpha_i]$ for all $i\in I_F$. Thus, $z_i^{TOP_F}(l_F)=z_{i-1}^{BOT_F}(l_F)=0$, or $z_i^{TOP_F}(x_F)=z_{i-1}^{BOT_F}(x_F)=0$, meaning that (1) x_F lies on the boundary of pinch simplex for sections TOP_F and BOT_F, and (2) both pinch simplices share the same boundaries. This will lead to the eigenvalue relationship for adjacent pinched column sections connected by a feed stream.

Now, let us consider Scenario 2, where the target separation goal can be achieved in the column sections using just a finite number of stages. This happens when V^{TOP_F} increases above its minimum threshold (i.e., Scenario 1), and thus $\gamma_i^{TOP_F}>\rho_{i-1,F}>\gamma_{i-1}^{BOT_F}$ for every $i\in I_F$ due to the monotonicity of Equation (10) with respect to $\gamma\in[\alpha_{i-1},\alpha_i]$.

Recall that the scaling factor r_i in Equations (15) and (16) has the same sign as d_i. Thus, for every $i\in I_F$, $r_i^{TOP_F}$ is positive and $r_i^{BOT_F}$ is negative. Therefore, with an increased V^{TOP_F} value, both $z_i^{TOP_F}(x_F)=r_i^{TOP_F}\left(\omega^T\right)_i^{TOP_F}x_F$ and $z_{i-1}^{BOT_F}(x_F)=r_{i-1}^{BOT_F}\left(\omega^T\right)_{i-1}^{BOT_F}x_F$ would increase and become positive. Likewise, in Scenario 3, where the target separation goal cannot be achieved even with infinite stages in the column sections, V^{TOP_F} decreases to less than its value in Scenario 1. One can show that $\gamma_i^{TOP_F}<\rho_{i-1,F}<\gamma_{i-1}^{BOT_F}$ for every $i\in I_F$, and both $z_i^{TOP_F}(x_F)$ and $z_{i-1}^{BOT_F}(x_F)$ would decrease and become negative.

A similar analysis can be drawn for liquid-only feed stream as well. To summarize, given a two-phase or a liquid-only feed stream F, for all $i\in I_F$ determined from Equation (30), its liquid flow composition x_F satisfies one of the following three scenarios:

$$\begin{aligned}&\text{Scenario 1}:z_i^{TOP_F}(x_F)=z_{i-1}^{BOT_F}(x_F)=0,\\&\text{Scenario 2}:z_i^{TOP_F}(x_F)>0,z_{i-1}^{BOT_F}(x_F)>0,\\&\text{Scenario 3}:z_i^{TOP_F}(x_F)<0,z_{i-1}^{BOT_F}(x_F)<0.\end{aligned}\quad(33)$$

Figure 11 illustrates Equation (33) from a geometric perspective for the case of a simple column performing ternary separation. Essentially, the hyperplane $z_i^{TOP_F}(x)=0$ (resp. $z_{i-1}^{BOT_F}(x)=0$), which contains one of the facets of pinch simplex for section TOP_F (resp. BOT_F), divides $\mathbb{R}^{c-1}$ into two half-spaces, one of which contains the entire pinch simplex. If x_F lies in the closed half-space containing (resp. not containing) TOP_F pinch simplex, it must also lie in the closed half-space containing (resp. not containing) BOT_F pinch simplex, and vice versa. In particular, if x_F lies on the hyperplane $z_i^{TOP_F}(x)=0$, it must also lie on the hyperplane $z_{i-1}^{BOT_F}(x)=0$ for all $i\in I_F$, and vice versa. In essence, *this is the geometric interpretation of the classic Underwood method.*[54]
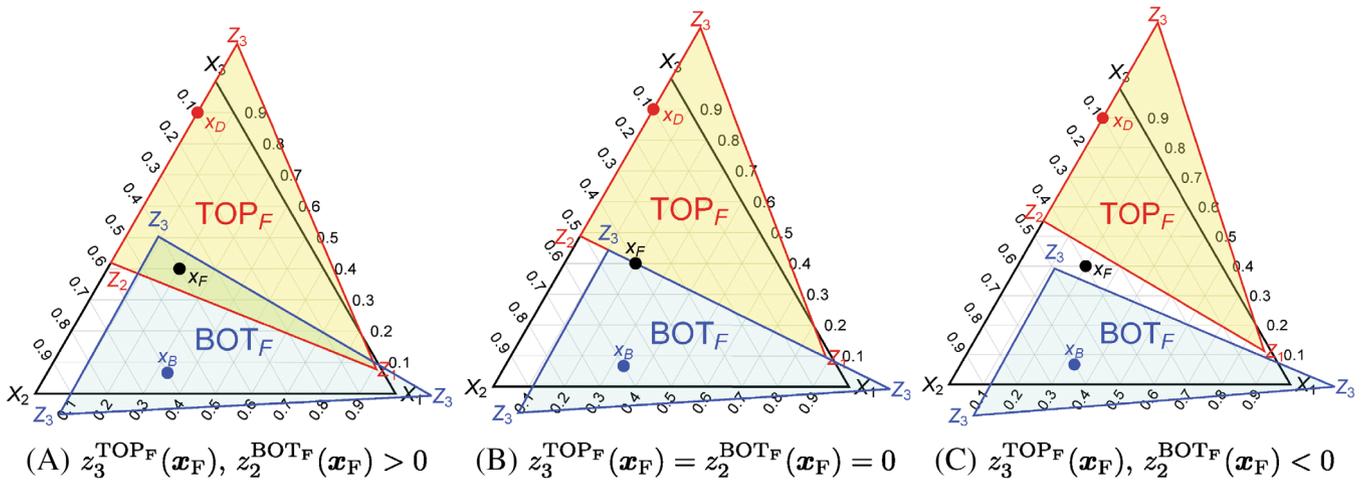
For a vapor-only feed stream F, it can be shown that the hypothetical liquid composition, $\widetilde{x}_F$, which would be in thermodynamic equilibrium with the vapor feed v_F via Equation (2), satisfies one of the following three scenarios:

$$\begin{aligned}&\text{Scenario 1}:z_i^{TOP_F}(\widetilde{x}_F)=z_{i-1}^{BOT_F}(\widetilde{x}_F)=0,\\&\text{Scenario 2}:z_i^{TOP_F}(\widetilde{x}_F)>0,z_{i-1}^{BOT_F}(\widetilde{x}_F)>0,\\&\text{Scenario 3}:z_i^{TOP_F}(\widetilde{x}_F)<0,z_{i-1}^{BOT_F}(\widetilde{x}_F)<0.\end{aligned}\quad(34)$$

Furthermore, we conclude that, in order for sections TOP_F and BOT_F to successfully perform the target separation task, which corresponds to Scenarios 1 and 2, the section γ roots obtained by solving Equation (10) must satisfy the following feasibility condition:

$$\gamma_i^{TOP_F}\geq\rho_{i-1,F}\geq\gamma_{i-1}^{BOT_F}\quad\forall i\in I_F,\quad(35)$$

where the equality holds when the two column sections are pinched. *This is a key result that ensures feasibility of a given separation task in adjacent column sections connected by a feed stream.* We note that all possible ρ_i roots for $i\in\{1,\cdots,c-1\}$ typically can be determined a priori by solving Equation (31) or (32), as the feed specifications are generally known to us. Also, we want to point out that Equations (31) and (32) become the classic Underwood feed equations when considering simple columns (see Figure 11).[39] And these ρ roots are

(A) $z_3^{\mathrm{TOP_F}}(\boldsymbol{x}_F), z_2^{\mathrm{BOT_F}}(\boldsymbol{x}_F) > 0$ (B) $z_3^{\mathrm{TOP_F}}(\boldsymbol{x}_F) = z_2^{\mathrm{BOT_F}}(\boldsymbol{x}_F) = 0$ (C) $z_3^{\mathrm{TOP_F}}(\boldsymbol{x}_F), z_2^{\mathrm{BOT_F}}(\boldsymbol{x}_F) < 0$

FIGURE 11   In this example, we consider a ternary mixture distillation in a simple column with $(\alpha_1, \alpha_2, \alpha_3) = (1, 2.25, 3)$. The saturated liquid feed flow rate is $(f_{1,F}, f_{2,F}, f_{3,F}) = (0.2, 0.4, 0.4)$, and the distillate flow rate is $\left(d_1^{\mathrm{TOP_F}}, d_2^{\mathrm{TOP_F}}, d_3^{\mathrm{TOP_F}}\right) = (0, 0.04, 0.36)$. Since $p^{\mathrm{TOP_F}} = 2$ and $p^{\mathrm{BOT_F}} = 3$ in this case, $I_F = \{3\}$. (A) Scenario 2 of Equation (33): When $V^{\mathrm{TOP_F}} = V^{\mathrm{BOT_F}} = 2.7 > 2.2972$, the liquid composition of the feed stream $\boldsymbol{x}_F = l_F/L_F$ lies in the interior in the pinch simplex of both rectifying ($\mathrm{TOP_F}$) and stripping ($\mathrm{BOT_F}$) sections; (B) Scenario 1: When $V^{\mathrm{TOP_F}} = V^{\mathrm{BOT_F}} = 2.2972$, $\boldsymbol{x}_F$ lies on the facet of both pinch complices; (C) Scenario 3: When $V^{\mathrm{TOP_F}} = V^{\mathrm{BOT_F}} = 2.0 < 2.2972$, $\boldsymbol{x}_F$ is outside of both pinch simplices, the separation is infeasible.

essentially the Underwood roots. As a result, the well-known Underwood method is just a special case of Equation (35), where the inequality constraints (Scenarios 1 and 2) reduce to equalities (Scenario 1).

5.2 | Identifying eigenvalue relationships for adjacent column sections connected by a sidedraw stream

When two infinite column sections are connected by a sidedraw stream, the analysis approach follows similarly as before. Here, we summarize the key results. Suppose the actual pinch zone liquid compositions in $\mathrm{TOP_W}$ and $\mathrm{BOT_W}$ correspond to $\boldsymbol{Z}_p^{\mathrm{TOP_W}}$ and $\boldsymbol{Z}_p^{\mathrm{BOT_W}}$, respectively. Then the associated pinch eigenvalues are respectively denoted as $\lambda_p^{\mathrm{TOP_W}}$ and $\lambda_p^{\mathrm{BOT_W}}$. Since a sidedraw stream takes materials out of the column, $\boldsymbol{d}^{\mathrm{TOP_W}} - \boldsymbol{d}^{\mathrm{BOT_W}} = \boldsymbol{v}_W + \boldsymbol{l}_W < \boldsymbol{0}$, and thus $p^{\mathrm{TOP_W}} \geq p^{\mathrm{BOT_W}}$. With this, we define an index set I_W based on Proposition 3 as:

$$I_W = \left\{ i \in C, \lambda_i^{\mathrm{BOT_W}} > \lambda_p^{\mathrm{BOT_W}} \big| \lambda_{i-1}^{\mathrm{TOP_W}} < \lambda_p^{\mathrm{TOP_W}} \right\} = \left\{ p^{\mathrm{BOT_W}} + 1, \cdots, p^{\mathrm{TOP_W}} \right\}. \tag{36}$$

with $d_i^{\mathrm{BOT_W}} > 0$ and $d_{i-1}^{\mathrm{TOP_W}} < 0$ simultaneously satisfied for all $i \in I_W$. Again, depending on the value of section vapor flow $V^{\mathrm{TOP_W}}$ (or $V^{\mathrm{BOT_W}}$), exactly one of the following three scenarios will occur: (1) column sections are pinched, which requires an infinite number of stages in the sections to achieve the target separation goal; (2) target separation can be achieved in the column sections using a finite number of stages; (3) target separation cannot be achieved even with an infinite

number of stages. In addition, as shown in Figure 10B, $\boldsymbol{v}_W$, $\boldsymbol{v}_1^{\mathrm{BOT_W}}$, and $\boldsymbol{v}_0^{\prime\mathrm{TOP_W}}$ all have the same composition, so do $\boldsymbol{l}_W$, $\boldsymbol{l}_1^{\prime\mathrm{TOP_W}}$, and $\boldsymbol{l}_0^{\mathrm{BOT_W}}$. It can be shown that the sidedraw composition presents a similar result as in Equations (33) and (34). Specifically, if sidedraw W is a two-phase or a liquid-only stream, for all $i \in I_W$ determined from Equation (36), its liquid flow composition $\boldsymbol{x}_W$ will fall in with one of the following three scenarios:

$$
\begin{aligned}
&\text{Scenario 1.} \ z_{i-1}^{\mathrm{TOP_W}}(\boldsymbol{x}_W) = z_i^{\mathrm{BOT_W}}(\boldsymbol{x}_W) = 0, \\
&\text{Scenario 2.} \ z_{i-1}^{\mathrm{TOP_W}}(\boldsymbol{x}_W) > 0, z_i^{\mathrm{BOT_W}}(\boldsymbol{x}_W) > 0, \\
&\text{Scenario 3.} \ z_{i-1}^{\mathrm{TOP_W}}(\boldsymbol{x}_W) < 0, z_i^{\mathrm{BOT_W}}(\boldsymbol{x}_W) < 0.
\end{aligned} \tag{37}
$$

On the other hand, if sidedraw W is a vapor-only stream, the hypothetical liquid composition, $\widetilde{\boldsymbol{x}}_W$, which would be in thermodynamic equilibrium with $\boldsymbol{v}_W$, will fall in with one of the three scenarios below, for every $i \in I_W$:

$$
\begin{aligned}
&\text{Scenario 1.} \ z_{i-1}^{\mathrm{TOP_W}}(\widetilde{\boldsymbol{x}}_W) = z_i^{\mathrm{BOT_W}}(\widetilde{\boldsymbol{x}}_W) = 0, \\
&\text{Scenario 2.} \ z_{i-1}^{\mathrm{TOP_W}}(\widetilde{\boldsymbol{x}}_W) > 0, z_i^{\mathrm{BOT_W}}(\widetilde{\boldsymbol{x}}_W) > 0, \\
&\text{Scenario 3.} \ z_{i-1}^{\mathrm{TOP_W}}(\widetilde{\boldsymbol{x}}_W) < 0, z_i^{\mathrm{BOT_W}}(\widetilde{\boldsymbol{x}}_W) < 0.
\end{aligned} \tag{38}
$$

Furthermore, we conclude that, in order for sections $\mathrm{TOP_W}$ and $\mathrm{BOT_W}$ to successfully carry out the target separation (Scenarios 1 and 2), the γ roots obtained by solving Equation (10) must satisfy the following feasibility condition:

$$\gamma_{i-1}^{\mathrm{TOP_W}} \leq \rho_{i-1,W} \leq \gamma_i^{\mathrm{BOT_W}} \quad \forall i \in I_W, \tag{39}$$

where $\rho_{i-1,W} \in [\alpha_{i-1}, \alpha_i]$ for every $i \in I_W$ is defined for the sidedraw stream W as the solution of the following equations analogous to Equations (31) and (32):

$$\sum_{j=1}^{c} \frac{\alpha_j l_{j,W}}{\alpha_j - \rho_{i-1,W}} = 0, \quad \sum_{j=1}^{c} \frac{\alpha_j v_{j,W}}{\alpha_j - \rho_{i-1,W}} = V_W, \quad \sum_{j=1}^{c} \frac{\alpha_j f_{j,W}}{\alpha_j - \rho_{i-1,W}} = V_W. \quad (40)$$

Similar to Equations (35), Equation (39) is a key result that ensures feasibility of a given separation task in two neighboring column sections connected by a sidedraw. Furthermore, to the best of our knowledge, despite its similarity with Equation (31) and (32) defined for feed stream, Equation (40), which is related to sidedraw W, has not been explored or reported in the literature. In this way, our shortcut model greatly extends the classic Underwood method by discovering new constraints needed for characterizing sidedraw streams. Note that analogous to Equation (35), the inequalities in Equation (39) reduce to equalities when the two column sections are pinched in order to carry out the target separation task (Scenario 1).

6 | MINIMUM REFLUX CONDITION

In earlier sections, we developed understanding of composition profile in a single column section based on pinch simplex. We also derived algebraic constraints describing the feasibility of target separation task in adjacent column sections connected by either a feed or sidedraw stream. Generalizing these findings to derive minimum reflux conditions for an MFMP column is as easy as stacking back each individual column sections and checking the eigenvalue relationship (Equations 35 or 39) for every column section pair to ensure that the section vapor flow leads to feasible separation for every column section. Suppose an MFMP column has N_{SEC} sections, then the minimum reboiler duty requirement (resp. minimum reflux ratio) of the MFMP column is then the lowest reboiler vapor duty (resp. lowest reflux ratio) satisfying all $N_{SEC} - 1$ such eigenvalue relationships, one for each column section pair. Given feed and product stream specifications (flow rate, composition, thermal quality), the determination of minimum reboiler vapor duty or minimum reflux ratio can be implemented as an algorithmic procedure as follows:

1. From the given feed and product specifications, calculate d_i^{Seck} for every component $i \in C$ and every column section $k = 1, \cdots, N_{SEC}$.
2. From Equation (25) and Proposition 3, determine pinch index p^{Seck} for every section $k = 1, \cdots, N_{SEC}$. Then, for each feed stream $j = 1, \cdots, N_F$ and sidedraw stream $s = 0, \cdots, N_W$ involved, determine the corresponding index set I_{F_j} or I_{W_s} using Equation (30) or (36).
3. For every feed stream $j = 1, \cdots, N_F$, solve Equation (31) or (32) to obtain roots ρ_{i-1,F_j} for every $i \in I_{F_j}$ (provided that $I_{F_j} \neq \emptyset$). Similarly, for every sidedraw stream $s = 0, \cdots, N_W$ present, obtain ρ_{i-1,W_s} roots from Equation (40) for every $i \in I_{W_s}$ (provided that $I_{W_s} \neq \emptyset$).
4. For every ρ_{i-1,F_j} (resp. ρ_{i-1,W_s}) obtained, let $\gamma_i^{TOP_{F_j}} = \rho_{i-1,F_j}$ (resp. $\gamma_{i-1}^{TOP_{W_j}} = \rho_{i-1,W_j}$) and calculate section vapor flow $V^{TOP_{F_j}}$ (resp. $V^{TOP_{W_j}}$) using Equation (10). Then, substitute this $V^{TOP_{F_j}}$ (resp. $V^{TOP_{W_j}}$) value into Equation (29) to obtain section vapor flow V^{Seck} for all $k = 1, \cdots, N_{SEC}$.

5. For every adjacent column section pair ($k = 1, \cdots, N_{SEC} - 1$), using the corresponding section vapor flows V^{Seck} and V^{Seck+1} obtained from the previous step, determine section γ roots from Equation (10), and verify if the feasibility conditions of Equations (35) and (39) are satisfied. If the feasibility conditions are satisfied for all adjacent column section pairs in the MFMP column, store the bottommost section vapor flow $V^{SecN_{SEC}}$ and the reflux ratio $R = \frac{V^{Sec1}}{D} - 1$.
6. The true minimum reboiler vapor duty requirement and minimum reflux ratio of the MFMP column correspond to the lowest $V^{SecN_{SEC}}$ and R values stored, respectively.

It is worth mentioning again that the algorithmic procedure above applies when the feed and product specifications are provided. Sometimes, however, some of the specifications may not be known to users a priori. For example, users may only require certain components to be within a specific purity limit in a product stream. In this case, determining the minimum reboiler vapor duty or minimum reflux ratio actually becomes an optimization problem. When it is correctly formulated and solved, the optimization program will determine the remaining stream specifications such that the reboiler vapor duty or reflux ratio is minimized globally. In Part 2 of this series, we will present the detailed optimization formulation and solution strategies that implement the new shortcut method developed here. Next, we would like to shed some light on the accuracy and attractiveness of our new shortcut method by walking through a simple illustrative example.

6.1 | An illustrative example

We consider a two-feed distillation column shown in Figure 12A separating mixtures of n-octane (Component 1), n-heptane (Component 2), and n-hexane (Component 3), where $(\alpha_1, \alpha_2, \alpha_3) = (1, 2.2500, 5.1168)$. Both feed streams enter the column in saturated liquid state. The composition and flow rate for all streams are listed in Table 2. After calculating the net material upward flow rate for each column section, we determine from Equation (25) and Proposition 3 that the pinch indices are $p^{Sec1} = p^{Sec2} = 2$ and $p^{Sec3} = 3$ for all three sections. Therefore, from Equation (30), we get $I_{F_1} = \emptyset$ and $I_{F_2} = \{3\}$. This means that Sections 2 and 3 are pinched during minimum reflux operation. To obtain the minimum reflux ratio, we simply calculate $\rho_{2,F_2} = 3.6186 \in [\alpha_2, \alpha_3]$ from Equation (31), and let $\gamma_3^{Sec2} = \rho_{2,F_2} = \gamma_2^{Sec3}$ due to Equation (35). The corresponding minimum reboiler vapor duty requirement is determined to be 140.81 mol/s by substituting $\gamma_3^{Sec2} = \gamma_2^{Sec3} = 3.6186$ into Equations (10) and (29). The corresponding minimum reflux ratio calculated is 1.683. Figure 12B shows the pinch simplices at minimum reflux.

Rigorous Aspen Plus simulation result predicts the minimum reflux ratio to be 1.735, which is only less than 3% different from that calculated using our shortcut method. While this result itself already shows the accuracy of our shortcut method, what makes this new method more powerful is that, when we instead rely on the commonly used column decomposition method (Figure 2), we would have chosen
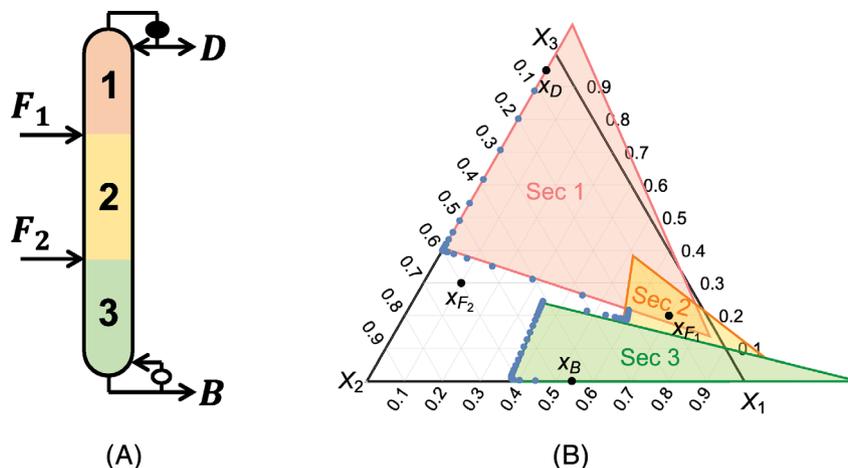
FIGURE 12 An illustrative example considering ternary mixture separation in a two-feed column. Note that in (B), minimum reflux is achieved when the pinch simplex of intermediate column section (Section 2) share the common edge with the pinch simplex of the bottommost section (Section 3). Therefore, at minimum reflux, Sections 2 and 3 are pinched, and the lower feed composition x_{F_2} lies on this common edge (i. e., $z_3^{Sec2}(x_{F_2}) = z_2^{Sec3}(x_{F_2}) = 0$). The blue dots in (B) are the actual liquid composition profile of this two-feed column simulated in Aspen Plus V12.1 as a RadFrac column. (A) A two-feed distillation column; (B) Pinch simplices at true minimum reflux.

TABLE 2 Feed and product specifications for the two-feed column of Figure 12A

Streams	Flow rate (mol/s)	Molar composition (x_3, x_2, x_1)
D	52.476	(0.95, 0.05, trace)
F_1	100	(0.2, 0.1, 0.7)
F_2	100	(0.3, 0.6, 0.1)
B	147.524	(0.001, 0.4567, 0.5423)

Note: Hexane composition in the bottoms product stream is small (0.001) but not in trace amount.

the largest minimum reflux ratio value obtained by the classic Underwood method applied to the decomposed columns to be our "minimum reflux ratio" of the column. It turns out that the "minimum reflux ratio" determined from column decomposition approach is as high as 19.66, which is more than 11 times higher than the true minimum reflux! One can imagine the enormous scale of waste in energy consumption and capital expenditure if the column is designed and operated based on the column decomposition method. This simple example clearly illustrates the accuracy and attractiveness of this new shortcut approach. In Part 2 of the series, we will offer detailed discussions on why some of the commonly used modeling assumptions and heuristics, such as the column decomposition method, would fail for MFMP columns.

7 | CONCLUSION

Multi-feed, multi-product distillation columns are commonly used in many industrial separations. The minimum reflux ratio of a distillation column is related to its energy consumption and capital cost, and thus is a key parameter in distillation design. To solve this lingering problem of determining the minimum reflux ratio of a general MFMP

column in an accurate and computationally efficient manner, we follow a bottom-up modeling approach and develop a first-of-its-kind mathematical model for a general MFMP column based on ideal-VLE, CRV, and CMO assumptions. First, we focus on modeling a general column section, the basic module in a general MFMP column. To account for the nonlinearities caused by the ideal-VLE relations in the model, we propose a linearization technique that requires a variable transformation. By studying the eigenvalue problem resulting from the linear system, we find the analytical expression for the composition profile within the column section without the need to perform tedious tray-by-tray calculations. We relate the eigenvalues and eigenvectors with potential pinch conditions within the column section. We also explore the geometric interpretations of the eigenvalue problem after we introduce the concept of pinch simplex. Next, we explore several properties of the model as the column section becomes pinched, followed by analyzing how eigenvalues and pinch simplices characterizing any two adjacent column sections are related as the sections are stacked and connected by feed or sidedraw stream. Finally, we derive algebraic constraints for feasible separation and minimum reflux operation of an MFMP column, followed by explaining their geometric meaning. In the case of a simple column, the shortcut method developed in this work reduces to the classic Underwood method.[38]

As we have mentioned, this method uses the same underlying assumptions as the Underwood method.[39] We remark that the constant molar overflow (CMO) assumption implies that all components have similar latent heat of vaporization. However, it turns out that this assumption can be relaxed to account for cases in which components have very distinct latent heats, which can be quite common in practice. With only slight modification of Underwood's classic model,[38] this extension has been independently developed by Nandakumar and Andres[58] as well as Rev[59] for simple columns. The final expression, despite its great similarity compared to the Underwood equation,

directly calculates the heat duty requirement rather than vapor duty. We believe that the shortcut method developed in this article can also be extended in a similar manner to determine the minimum heat duty requirement of an MFMP column with unequal component latent heats of vaporization. Using a simple transformation of variables as introduced by Nandakumar and Andres[59] as well as Rev,[59] all the mathematical relationships and properties developed in this article still apply to the extended model. We leave the discussion of this extension to future work.

In Part 2 of the series, we will incorporate our new shortcut method into a global optimization framework. We will also analyze a number of case studies involving different MFMP column configurations that address the common misconceptions and doubts in multicomponent distillation systems design. Through these case studies, we will provide readers with answers to the questions raised at the beginning of this article.

PARAMETERS AND VARIABLES

c	total number of components present in the distillation column
α_i	relative volatility of component i with respect to the heaviest component
n	stage number following the convention of Figure 4
$v'_{i,n}$ (resp. $v_{i,n}$)	component i vapor flow leaving stage n in the lower (resp. upper) part of section
$l'_{i,n}$ (resp. $l_{i,n}$)	component i liquid flow leaving stage n in the lower (resp. upper) part of section
d_i	component i net material upward flow defined in Equation (1)
V	total vapor flow in the column section, $V = \mathbf{e}^T \mathbf{v}'_n = \mathbf{e}^T \mathbf{v}_{n+1}$ for every $n \in \mathbb{N}$
L	total liquid flow in the column section, $L = \mathbf{e}^T \mathbf{l}'_{n+1} = \mathbf{e}^T \mathbf{l}_n$ for every $n \in \mathbb{N}$
D	total net material upward flow, $D = V - L = \mathbf{e}^T \mathbf{d}$
$\mathbf{A}$	matrix $\mathbf{A}$ defined in Equation (6)
$\mathcal{L}'_{i,n}$	new variable defined in Equation (5) for the lower part of column section
λ_i	the ith eigenvalue of matrix $\mathbf{A}$ defined in Equations (9): $\lambda_c > \cdots > \lambda_1$
γ_i	the ith root of Equation (10), $\gamma_i = \lambda_i / V$
$\boldsymbol{\nu}_i$	the eigenvector of $\mathbf{A}$ associated with eigenvalue λ_i defined in Equation (12)
$\mathbf{Q}$	the eigenvector matrix of $\mathbf{A}$, $\mathbf{Q} = [\boldsymbol{\nu}_1, ..., \boldsymbol{\nu}_c]$
$\mathbf{Q}^{-1}$	the inverse matrix of eigenvector matrix $\mathbf{Q}$, with $\mathbf{Q}\mathbf{Q}^{-1} = \mathbf{A}$
ω_i^T	a row vector defined in Equations (15) and (16) that is related to $\mathbf{Q}^{-1}$
r_i	the scaling factor defined in Equations (15) and (16)
$\boldsymbol{\Lambda}$	the diagonal matrix whose diagonal elements contain all eigenvalues of $\mathbf{A}$
$\mathbf{x}'_n$ (resp. $\mathbf{y}'_n$)	the liquid (resp. vapor) composition vector in the lower part of column section
$\mathbf{x}_n$ (resp. $\mathbf{y}_n$)	the liquid (resp. vapor) composition vector in the upper part of column section
$\mathbf{z}(\mathbf{x})$	a linear transformation defined in Equation (18)
$z_i(\mathbf{x}) = 0$	the hyperplane equation associated with λ_i for constructing the pinch simplex
$\mathbf{e}_i$	a column unit vector in $\mathbb{R}^c$ with its ith element being 1 and the rest being 0
$\mathbf{e}$	an all-ones column vector with c elements in $\mathbb{R}^c$
X_i	the composition of pure component i in x- or z-space
Z_i	liquid pinch composition corresponding to $\boldsymbol{\nu}_i$ in x- or z-space
C_x, C_z	composition simplices drawn in x- space and z-space, respectively
P_x, P_z	pinch simplices drawn in x- space and z-space, respectively
$f'_n(x), f_n(x)$	functions in Equation (22) respectively for the lower and upper part of column section
$x'_k(n), x_k(n)$	the kth root of $f'_n(x) = 0$ and $f_n(x) = 0$ respectively for stage n
x'_k, x_k	the kth root of $f'_n(x) = 0$ and $f_n(x) = 0$ resp. as $n \to \infty$ in both parts of section
$C(x)$	a function defined in Equation (24)
v, l	the actual pinch zone vapor and liquid component flows, respectively
$F_1(x), F_2(x)$	functions defined in Equations (27) and (28), respectively
φ_i, ϕ_i	the ith root of $F_1(x) = 0$ and $F_2(x) = 0$, respectively
λ_p	the eigenvalue of matrix $\mathbf{A}$ associated with the actual pinch component liquid flow
$\mathbf{v}_F, \mathbf{l}_F$	component vapor and liquid flow rate of the feed stream
$\mathbf{v}_W, \mathbf{l}_W$	component vapor and liquid flow rate of the sidedraw stream
$\rho_{i,F}, \rho_{i,W}$	the ith common root defined in Equations (31) (or 32) and (40), respectively
N_{SEC}, N_F, N_W	total number of column sections, feed, and sidedraw streams, respectively

SETS AND NOTATIONS

C	$\{1, ..., c\}$
$\mathbb{N}, \mathbb{N}^+$	$\{0, 1, 2, ...\}$ and $\{1, 2, ...\}$, respectively
I_F	the index set defined in Equation (30) for identifying common roots $\theta_{i,F}$
I_W	the index set defined in Equation (36) for identifying common roots $\theta_{i,W}$
TOP_F	column section above a feed stream F
BOT_F	column section below a feed stream F
TOP_W	column section above a sidedraw stream W

BOT_W column section below a sidedraw stream W

F, W feed and sidedraw stream, respectively

AUTHOR CONTRIBUTIONS

Zheyu Jiang: Conceptualization (equal); data curation (lead); formal analysis (lead); investigation (lead); methodology (lead); resources (lead); software (lead); validation (lead); visualization (lead); writing – original draft (lead); writing – review and editing (lead). **Mohit Tawarmalani:** Conceptualization (equal); formal analysis (supporting); investigation (supporting); methodology (supporting); project administration (supporting); resources (supporting); software (supporting); supervision (equal); validation (supporting); visualization (supporting); writing – original draft (supporting); writing – review and editing (supporting). **Rakesh Agrawal:** Conceptualization (equal); data curation (supporting); formal analysis (supporting); funding acquisition (lead); investigation (supporting); methodology (supporting); project administration (lead); resources (supporting); software (supporting); supervision (lead); validation (supporting); visualization (supporting); writing – original draft (supporting); writing – review and editing (supporting).

ACKNOWLEDGMENT

DATA AVAILABILITY STATEMENT

Data sharing not applicable to this article as no datasets were generated or analyzed during the current study.

ORCID

Zheyu Jiang https://orcid.org/0000-0003-4747-0539

Rakesh Agrawal https://orcid.org/0000-0002-6746-9829

REFERENCES

1. Humphrey JL. Separation technologies: an opportunity for energy savings. *Chem Eng Prog*. 1992;88:32-42.

2. Górak A, Olujić Z. *Distillation: Fundamentals and Principles*. Elsevier; 2014.

3. Koehler J, Poellmann P, Blass E. A review on minimum energy calculations for ideal and nonideal distillations. *Ind Eng Chem Res*. 1995; 34(4):1003-1020.

4. Jiang Z, Agrawal R. Process intensification in multicomponent distillation: a review of recent advancements. *Chem Eng Res Des*. 2019;147: 122-145.

5. Jiang Z, Madenoor Ramapriya G, Tawarmalani M, Agrawal R. Process intensification in multicomponent distillation. *Chem Eng Trans*. 2018; 69:841-846.

6. Agrawal R, Tumbalam GR. Misconceptions about efficiency and maturity of distillation. *AIChE J*. 2020;66(8):e16294.

7. Shah VH, Agrawal R. A matrix method for multicomponent distillation sequences. *AIChE J*. 2010;56(7):1759-1775.

8. Petlyuk F, Platonov V, Slavinskii D. Thermodynamically optimal method for separating multicomponent mixtures. *Int Chem Eng*. 1965; 5(3):555-561.

9. Giridhar A, Agrawal R. Synthesis of distillation configurations: I. Characteristics of a good search space. *Comput Chem Eng*. 2010; 34(1):73-83.

10. Gilliland ER. Multicomponent rectification. *Ind Eng Chem*. 1940;32(8): 1101-1106.

11. Doherty MF. *Conceptual Design of Distillation Systems. McGraw-Hill Chemical Engineering Series*. McGraw-Hill; 2001.

12. Turton R, Bailie RC, Whiting WB, Shaeiwitz JA, Bhattacharyya D. *Analysis, Synthesis, and Design of Chemical Processes. Prentice-Hall International Series in the Physical and Chemical Engineering Sciences*. 4th ed. Prentice Hall; 2012.

13. Jiang Z, Mathew TJ, Zhang H, et al. Global optimization of multicomponent distillation configurations: global minimization of total cost for multicomponent mixture separations. *Comput Chem Eng*. 2019;126: 249-262.

14. Caballero JA, Grossmann IE. Design of distillation sequences: from conventional to fully thermally coupled distillation systems. *Comput Chem Eng*. 2004;28(11):2307-2329.

15. Fidkowski Z, Królikowski L. Minimum energy requirements of thermally coupled distillation systems. *AIChE J*. 1987;33(4):643-653.

16. Carlberg NA, Westerberg AW. Temperature-heat diagrams for complex columns. 2. Underwood's method for side strippers and enrichers. *Ind Eng Chem Res*. 1989;28(9):1379-1386.

17. Fidkowski ZT, Agrawal R. Multicomponent thermally coupled systems of distillation columns at minimum reflux. *AIChE J*. 2001;47(12):2713-2724.

18. Nallasivam U, Shah VH, Shenvi AA, Huff J, Tawarmalani M, Agrawal R. Global optimization of multicomponent distillation configurations: 2. Enumeration based global minimization algorithm. *AIChE J*. 2016;62(6):2071-2086.

19. Tumbalam Gooty R, Agrawal R, Tawarmalani M. An MINLP formulation for the optimization of multicomponent distillation configurations. *Comput Chem Eng*. 2019;125:13-30.

20. Erbar RC, Maddox RN. Minimum reflux rate for multicomponent distillation systems by rigorous plate calculations. *Can J Chem Eng*. 1962; 40(1):25-30.

21. Chien HHY. A rigorous method for calculating minimum reflux rates in distillation. *AIChE J*. 1978;24(4):606-613.

22. Tavana M, Hanson DN. The exact calculation of minimum flows in distillation columns. *Ind Eng Chem Process Des Dev*. 1979;18(1): 154-156.

23. Holland CD. *Fundamentals of Multicomponent Distillation. McGraw-Hill Chemical Engineering Series*. McGraw-Hill; 1981.

24. Taylor R, Krishna R, Kooijman H. Real-world modeling of distillation. *Chem Eng Prog*. 2003;98:28-39.

25. Lucia A, Amale A, Taylor R. Distillation pinch points and more. *Comput Chem Eng*. 2008;32(6):1342-1364.

26. Levy SG, Doherty MF. Design and synthesis of homogeneous azeotropic distillations. 4. Minimum reflux calculations for multiple-feed columns. *Ind Eng Chem Fundam*. 1986;25(2):269-279.

27. Koehler J, Aguirre P, Blass E. Minimum reflux calculations for nonideal mixtures using the reversible distillation model. *Chem Eng Sci*. 1991; 46(12):3007-3021.

28. Koehler J, Kuen T, Blass E. Minimum energy demand for distillations with distributed components and side-product withdrawals. *Chem Eng Sci*. 1994;49(19):3325-3330.

29. Julka V, Doherty MF. Geometric behavior and minimum flows for nonideal multicomponent distillation. *Chem Eng Sci*. 1990;45(7):1801-1822.

30. Lucia A, Taylor R. The geometry of separation boundaries: I. Basic theory and numerical support. *AIChE J*. 2005;52(2):582-594.

31. Gani R, Bek-Pedersen E. Simple new algorithm for distillation column design. *AIChE J*. 2000;46(6):1271-1274.

32. Fidkowski ZT, Malone MF, Doherty MF. Nonideal multicomponent distillation: use of bifurcation theory for design. *AIChE J*. 1991;37(12): 1761-1779.

33. Bausa J, Watzdorf RV, Marquardt W. Shortcut methods for nonideal multicomponent distillation: I. Simple columns. *AIChE J*. 1998;44(10): 2181-2198.

34. Danilov RY, Petlyuk FB, Serafimov LA. Minimum-reflux regime of simple distillation columns. *Theor Found Chem Eng*. 2007;41(4):371-383.

35. Rooks RE, Malone MF, Doherty MF. A geometric design method for side-stream distillation columns. *Ind Eng Chem Res*. 1996;35(10):3653-3664.

36. Von Watzdorf R, Bausa J, Marquardt W. Shortcut methods for nonideal multicomponent distillation: 2. Complex columns. *AIChE J*. 1999;45(8):1615-1628.

37. Skiborowski M, Recker S, Marquardt W. Shortcut-based optimization of distillation-based processes by a novel reformulation of the feed angle method. *Chem Eng Res Des*. 2018;132:135-148.

38. Underwood AJV. Fractional distillation of multicomponent mixtures. *Chem Eng Prog*. 1948;44:603-614.

39. Underwood AJV. Fractional distillation of multicomponent mixtures. *Ind Eng Chem*. 1949;41(12):2844-2847.

40. Madenoor Ramapriya G, Selvarajah A, Jimenez Cucaita LE, Huff J, Tawarmalani M, Agrawal R. Short-cut methods versus rigorous methods for performance-evaluation of distillation configurations. *Ind Eng Chem Res*. 2018;57(22):7726-7731.

41. Jiang Z. A shortcut minimum reflux calculation method for distillation columns separating multicomponent homogeneous azeotropic mixtures. *Le Scientifique*. 2020;2020(1):17-25.

42. Barnes FJ, Hanson DN, King CJ. Calculation of minimum reflux for distillation columns with multiple feeds. *Ind Eng Chem Process Des Dev*. 1972;11(1):136-140.

43. Wachter JA, Ko TKT, Andres RP. Minimum reflux behavior of complex distillation columns. *AIChE J*. 1988;34(7):1164-1184.

44. Sugie H, Lu B. On the determination of minimum reflux ratio for a multicomponent distillation column with any number of side-cut streams. *Chem Eng Sci*. 1970;25(12):1837-1846.

45. Glinos KN, Malone MF. Design of sidestream distillation columns. *Ind Eng Chem Process Des Dev*. 1985;24(3):822-828.

46. Nikolaides I, Malone M. Approximate design of multiple-feed/sidestream distillation systems. *Ind Eng Chem Res*. 1987;26(9):1839-1845.

47. Ruiz-Marín LE, Ramírez-Corona N, Castro-Agüero A, Jiménez-Gutiérrez A. Shortcut design of fully thermally coupled distillation systems with post-fractionator. *Ind Eng Chem Res*. 2011;50(10):6287-6296.

48. Adiche C, Vogelpohl A. Short-cut methods for the optimal design of simple and complex distillation columns. *Chem Eng Res Des*. 2011;89(8):1321-1332. Special Issue on Distillation & Absorption.

49. Gómez-Castro FI, Rico-Ramírez V, Segovia-Hernández JG, Hernández-Castro S, González-Alatorre G, El-Halwagi MM. Simplified methodology for the design and optimization of thermally coupled reactive distillation systems. *Ind Eng Chem Res*. 2012;51(36):11717-11730.

50. Adiche C, Aissa BA. A generalized approach for the conceptual design of distillation columns with complex configurations. *Chem Eng Res Des*. 2016;109:150-170.

51. Jiang Z, Zewei C, Huff J, Shenvi AA, Tawarmalani M, Agrawal R. Global minimization of total exergy loss of multicomponent distillation configurations. *AIChE J*. 2019;65(11):e16737.

52. Jiang MRG, Tawarmalani M, Agrawal R. Minimum energy of multicomponent distillation systems using minimum additional heat and mass integration sections. *AIChE J*. 2018;64(9):3229-3553.

53. Acrivos A, Amundson NR. On the steady state fractionation of multicomponent and complex mixtures in an ideal cascade: Part 1—analytic solution of the equations for general mixtures. *Chem Eng Sci*. 1955;4(1):29-38.

54. Franklin N, Forsyth J. The interpretation of minimum reflux conditions in multi-component distillation. *Trans Inst Chem Eng*. 1953;31:S56-S81.

55. Fenske MR. Fractionation of straight-run Pennsylvania gasoline. *Ind Eng Chem*. 1932;24(5):482-485.

56. Kolokolnikov AG, Zhvanetskii IB, Platonov VM, Slinko MG. Is minimum reflux independent of the feed input model in a two-section column? *Dokl Akad Nauk SSSR*. 1982;264(3):656-660.

57. Kister H. *Distillation Design*. McGraw-Hill; 1992.

58. Nandakumar K, Andres RP. Minimum reflux conditions, part I: theory. *AIChE J*. 1981;27(3):450-460.

59. Rev E. The constant heat transport model and design of distillation columns with one single distributing component. *Ind Eng Chem Res*. 1990;29(9):1935-1943.